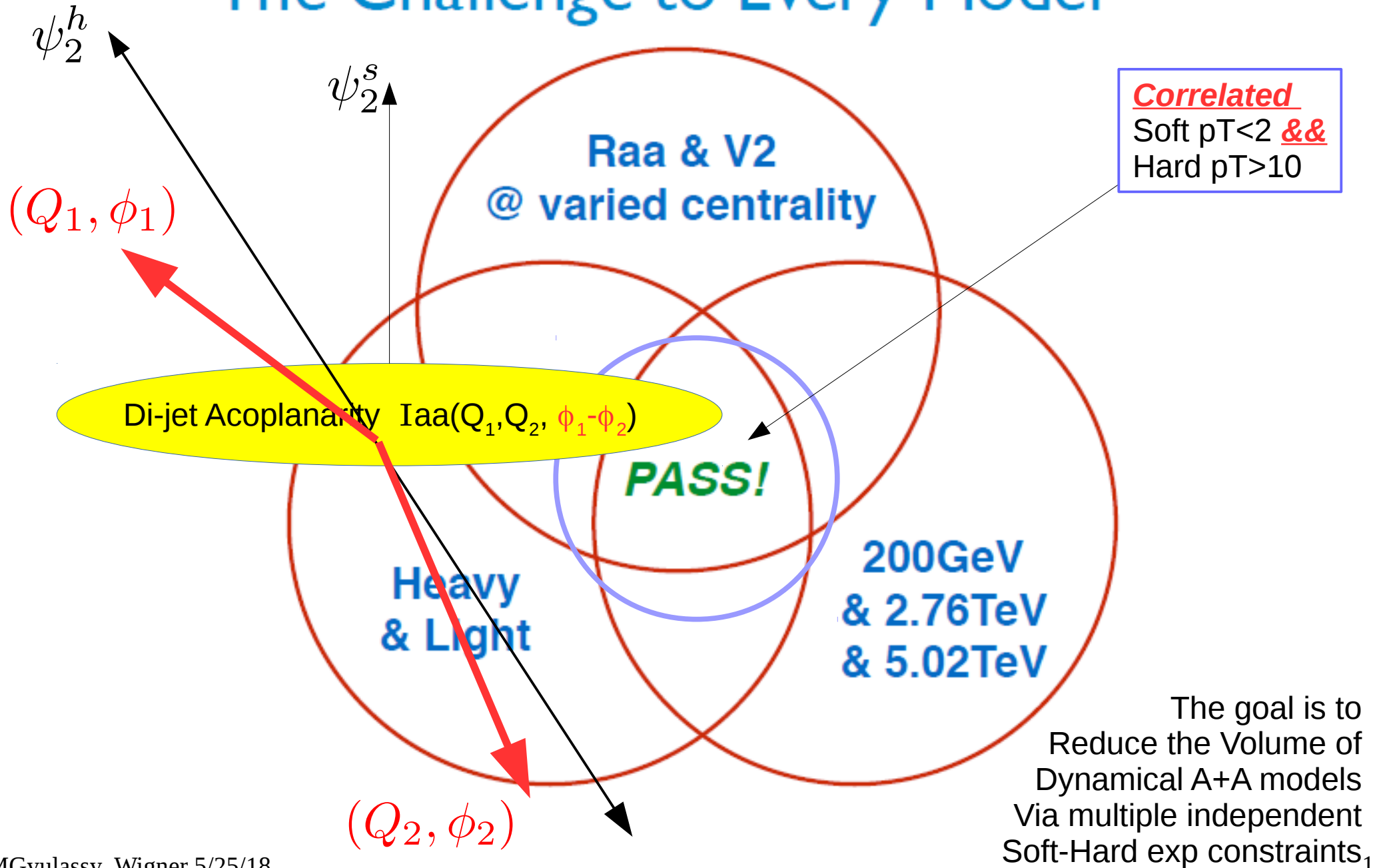


My QM18 talk focused on adding another exp observable, dijet acoplanarity, to Jinfeng Liao's QM17 list of correlated soft+hard tests that every model is now required to pass

The Challenge to Every Model



My interest in dijet acoplanarity was rekindled by Peter Jacobs' astute question at INT2017
Related to my talk on

Consistency of Perfect Fluidity and Jet Quenching in semi-Quark-Gluon-Monopole-Plasmas (sQGMP) [within the CUJET3.0 framework]

Jiechen Xu, J.Liao, MG, Chin.Phys.Lett. 32 (2015) and JHEP 1602 (2016) 169

Shuzhe Shi, J.Xu, J.Liao, MG, QM17

Shuzhe Shi, J.Liao, MG: arXiv:1804.01915

Probing the Color Structure of the Perfect QCD Fluids via Soft-Hard-Event-by-Event
Azimuthal Correlations [via our recent CIBJET= *ebe* VISHNU+CUJET3.1 framework]

My paraphrase of Peter Jacobs' question :

Can **future** higher precision dijet acoplanarity measurement be used to **falsify** sQGMP or wQGP
or AdS-BH models of jet-medium interactions in near perfect (unitarity bound) QCD fluids ?

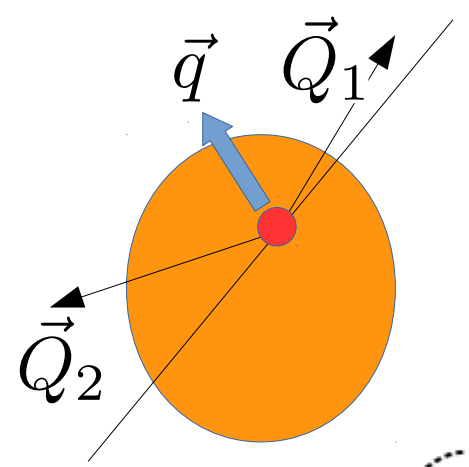
Or are dijet observables limited to the extraction of only one effective BDMS medium saturation
parameter that is insensitive to the microscopic color structure of QCD fluids??

$$Q_s^2(a) \equiv \left\langle q_\perp^2 \frac{L}{\lambda} \right\rangle_a \equiv \int dt \sum_b \hat{q}_{ab}(x(t), t) \equiv \sum_b \int dt d^2 q_\perp q_\perp^2 \Gamma_{ab}(q_\perp, t)$$

Can acoplanarity **distribution shapes** help to extract more information on the color d.o.f in the near
Perfect QCD fluids and on the microscopic differential scattering rates, Γ_{ab} , near $T \sim T_c$?

$$\Gamma_{ab}(q_\perp, T) = \rho_b(T) d^2 \sigma_{ab}(T) / d^2 q_\perp$$

h+Jet Acoplanarity $dN_{\text{bdms}}/d\Delta\phi$ vs $\Delta\phi$
 for Vac+BDMS $\alpha=0.09$ for $Q=20$ (solid), 60 (dots)
 $Q_s = 0$ (black), 3 (blue), 5 (red)



Dijet transverse acoplanarity momentum $\vec{q} = \vec{Q}_1 + \vec{Q}_2$

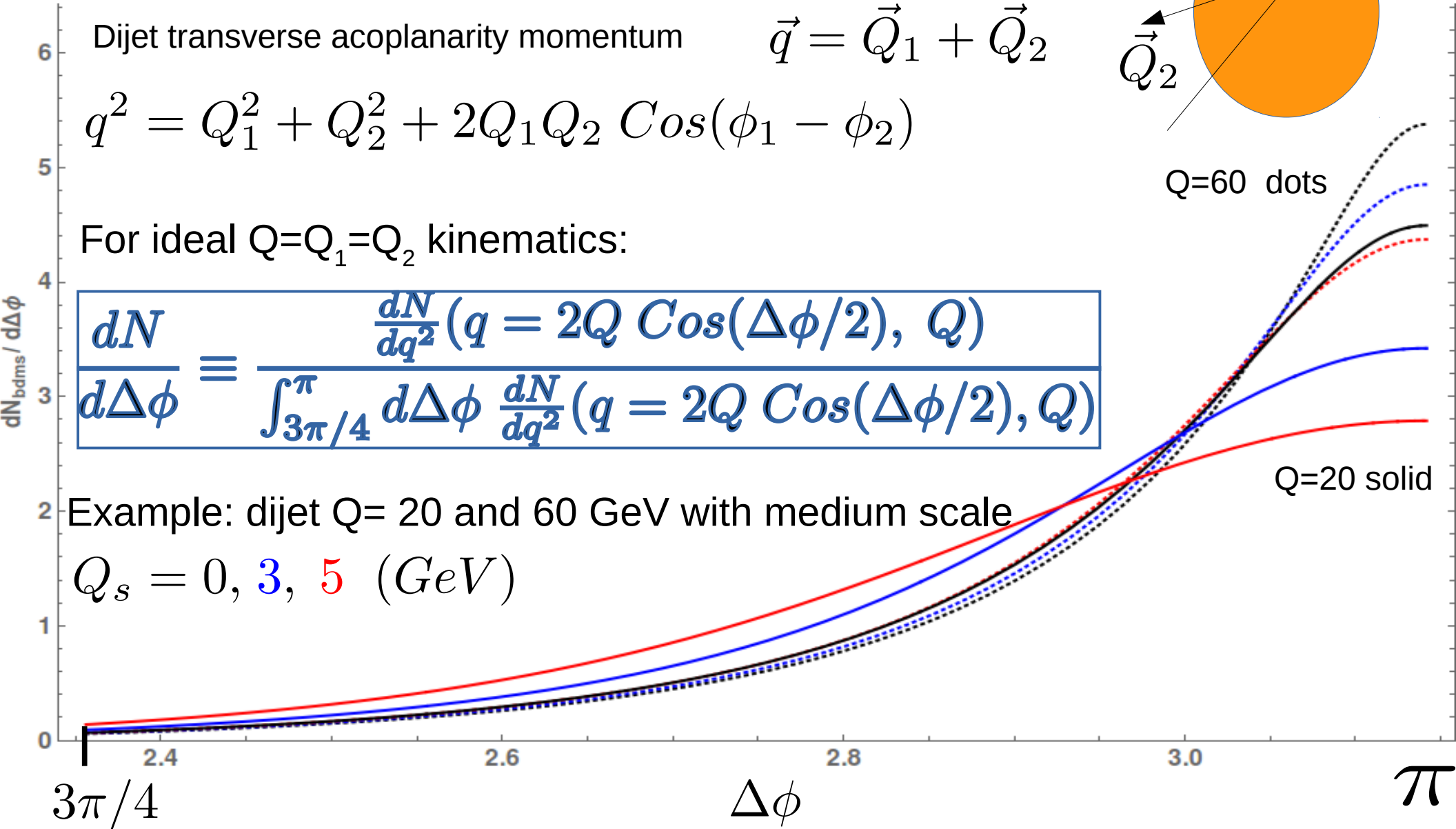
$$q^2 = Q_1^2 + Q_2^2 + 2Q_1Q_2 \cos(\phi_1 - \phi_2)$$

For ideal $Q=Q_1=Q_2$ kinematics:

$$\frac{dN}{d\Delta\phi} \equiv \frac{\frac{dN}{dq^2}(q = 2Q \cos(\Delta\phi/2), Q)}{\int_{3\pi/4}^{\pi} d\Delta\phi \frac{dN}{dq^2}(q = 2Q \cos(\Delta\phi/2), Q)}$$

Example: dijet $Q=20$ and 60 GeV with medium scale

$Q_s = 0, 3, 5$ (GeV)



State of the “acoplanarity art”

L. Chen et al. / Physics Letters B 773 (2017) 672–676

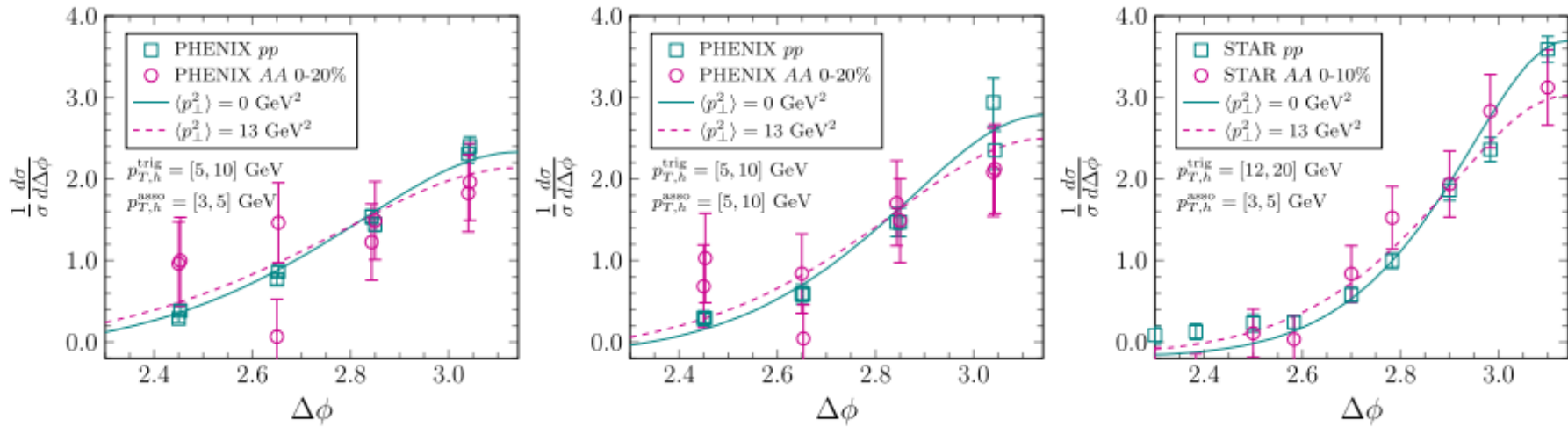


Fig. 1. Normalized dihadron angular correlation compared with PHENIX [51] and STAR [52] data.

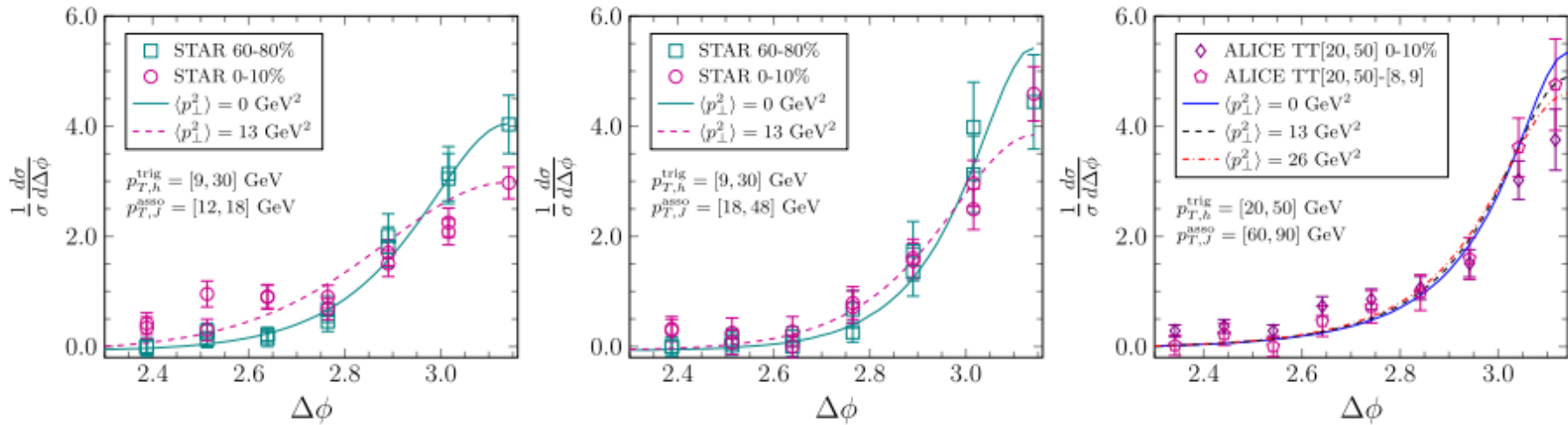


Fig. 2. Normalized hadron-jet angular correlation compared with STAR [53] and the ALICE [54] data. A factor of 3/2 is multiplied to the charged jet energy for our calculation to account for the energy carried by neutral particles. Two sets of ALICE data are shown: TT(trigger track)[20–50] (GeV) represents the signal and TT[20–50] (GeV)–[8–9] (GeV) subtracts the reference to suppress the contribution from the uncorrelated background.

[MG: Current exp precision does not constrain medium opacity better than RAA(pT), but much higher precision future data could test microscopic structure $n_a(T)$ and $d\sigma_{ab}/dq^2$]

(Acoplanarity of) **Jets as a probe of quark-gluon plasmas** (has a long history)

David A. Appel

Institute for Theoretical Physics, State University of New York at Stony Brook, Stony Brook, New York 11794

(Received 29 August 1985)

We investigate the propagation of jets through a quark-gluon plasma. The transverse-momentum imbalance of a jet pair is shown to be sensitive to multiple scattering off the constituents of the plasma for expected values of the plasma temperature and size. This raises the possibility that such transverse-momentum imbalance could be used as a probe of a quark-gluon plasma produced by partonic interactions in ultrarelativistic nucleus-nucleus collisions.

Jets in expanding quark-gluon plasmas

J. P. Blaizot

Service de Physique Theorique, CEA Saclay, 91191 Gif-sur-Yvette, Cedex, France

Larry D. McLerran

In summary, our analysis supports Appel's conclusion that jets may provide a useful diagnostic tool for studying the quark-gluon plasma. We have shown that in high-energy nuclear collisions, the effects of jet rescattering do in fact appear in the acoplanarity distribution. The cross section for scattering from the plasma may be inferred.

We should be careful to note, however, that the existence of acoplanarity does not by itself alone give evidence for a quark-gluon plasma, and may in fact be generated by scattering from a hadronic gas. The jet acoplanarity is therefore not a signal for the plasma, merely a diagnostic

M. Rammerstorfer and U. Heinz, (1990):" We find serious hadronic background effects from the surrounding nuclear matter in nuclear collisions, which severely limit the usefulness of jet acoplanarity as a quark-gluon-plasma probe. "

D.Appel 1986

J.P.Blaizot, L.McLerran(1986); M. Greco,(1985); ... V. Sudakov (1956)

Acoplanarity in Vacuum is due to Gluon radiation from dijet antenna

In the parton model there are no bremsstrahlung effects, so we have simply $dP/dK_\eta = \delta(K_\eta)$. With perturbative QCD, multiple gluon emission from the hard scattering can be resummed in perturbation theory,¹⁴ and for the one-dimensional normal momentum density has the form

$$\frac{1}{\sigma_0(p,p_T)} \frac{1}{p_T} \frac{d\sigma}{d\phi} = \frac{dP}{dK_\eta} = \frac{1}{\pi} \int_0^\infty db \cos(K_\eta b) \exp[\tilde{B}(b)] .$$

In Double leading log Sudakov approx

$$\tilde{B}(b) = - \int_{(b_0/b)^2}^{Q^2} \frac{dq^2}{q^2} \left[\ln \left[\frac{Q^2}{q^2} \right] A'(\alpha_s(q)) + B'(\alpha_s(q)) \right]$$

Additional acoplanarity in A+A arises from Jet-medium multiple scattering probability

$$F(\ell_T) \propto d\sigma / d^2 \ell_T$$

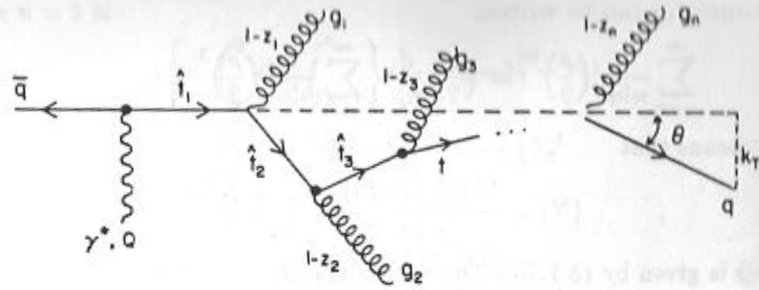
$$\frac{dP}{dK_\eta} = \sum_{n=0}^\infty \sum_{m=0}^\infty \left[\frac{1}{n!} \prod_{i=1}^n \int d^2 k_{Ti} B(\mathbf{k}_{Ti}) \frac{1}{m!} \prod_{j=1}^m \int d^2 l_{Tj} F(l_{Tj}) \delta \left[K_\eta - \sum_{i=1}^n (\mathbf{k}_{Ti})_\eta - \sum_{j=1}^m (l_{Tj})_\eta \right] \right]$$

$$\int_{-\infty}^{+\infty} dK_\eta \exp(iK_\eta b) \frac{dP}{dK_\eta} = \exp[\tilde{B}(b) + \tilde{F}(b)]$$

Exact trans mom conservation is easiest To enforce in conjugate b-space

Jet Acoplanarity in Vacuum is due to multiple small angle and soft gluon radiation

R.D.Fields, Applications of QCD, 1989



$S(\theta)$ = the probability that the quark created in the decay $\gamma^* \rightarrow q\bar{q}$ is diverted from its initial direction (opposite the antiquark) by an angle less than θ by successive

$$\frac{1}{\sigma_0} \left(\frac{d\sigma}{dk_T^2} \right)_{LDLA} = -\frac{4\alpha_s}{3\pi} \frac{1}{k_T^2} \log(k_T^2/Q^2) \exp \left\{ -\frac{2\alpha_s}{3\pi} \log^2(k_T^2/Q^2) \right\}$$

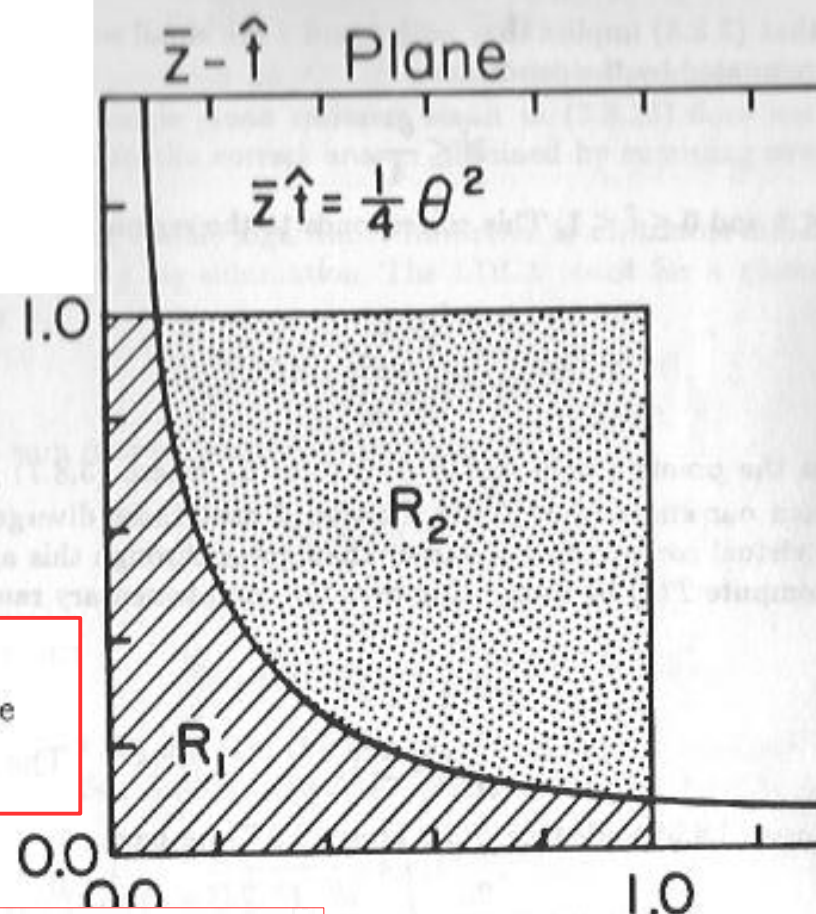


Figure 3.11 Shows the $\bar{z} - \hat{i}$ plane, where $\bar{z} = 1 - z$. The solid curve is $\bar{z}\hat{i} = \theta^2/4$ and R_1 is the region of integration for $S(\theta)$. The complementary region R_2 is the range of integration for $T(\theta)$ and $S(\theta) + T(\theta) = 1$.

Leading Double Log Approximation **Vanishes** at $k_T=0$ and at $k_T=Q$

Momentum conservation via b-space Leads to finite $q=0$ limit

Fig. 3.2 and to arrive at what will turn out to be the leading double logarithm we can use the LPA approximation in (3.4.10),

$$\frac{1}{\sigma_0} \left(\frac{d\sigma}{dzd\hat{i}} \right)_{LPA} = \frac{2\alpha_s}{3\pi} \frac{1+z^2}{(1-z)\hat{i}} \quad (3.8.7)$$

This term dominates since the range of integration for $S(\theta)$ is from (3.4.6) given by

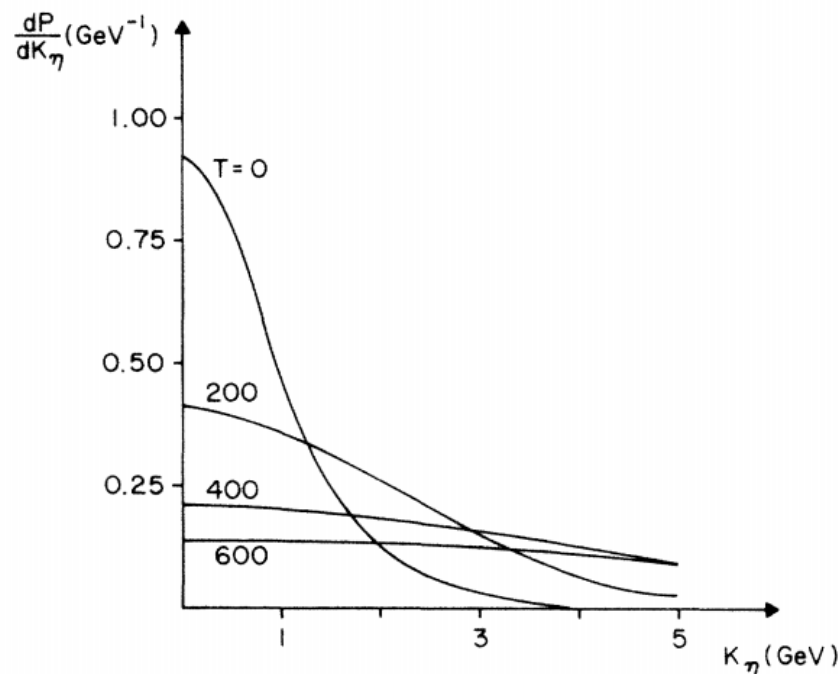
$$\frac{k_T^2}{Q^2} = z(1-z)\hat{i} \leq \frac{\theta^2}{4}, \quad (3.8.8)$$

For $F(l_T)$, the probability density for scattering elastically off the plasma constituents with transverse-momentum transfer l_T , we propose the following form:

$$F(l_T) = \sum_x n_x R \frac{d^2\sigma_x}{d^2l_T}, \quad (11)$$

where x runs over the different particle types comprising the plasma ($x = g, q_i, \bar{q}_i$), with n_x their number density. This equation essentially relates the plasma mean free path to the available distance for scattering (R) for each particular l_T .

Stefan-Boltzmann wQGP model estimates



$$F(l_T) = 9aRT^3 \left[1 + \frac{N_F}{4} \right] \frac{\alpha_s^2(l_T)}{l_T^4}$$

Cut off soft divergence below pQCD Debye mass

$$\ell_{\perp} \sim gT$$

“Based on this, one is encouraged to conjecture that someday jet behavior could be used as an effective thermometer of a QCD plasma.”

Confirmed by J.P.Blaizot, L.McLerran(1986)
In more realistic detail

Medium Induced Acoplanarity Distribution shapes due to multiple collisions depend on at least two parameters

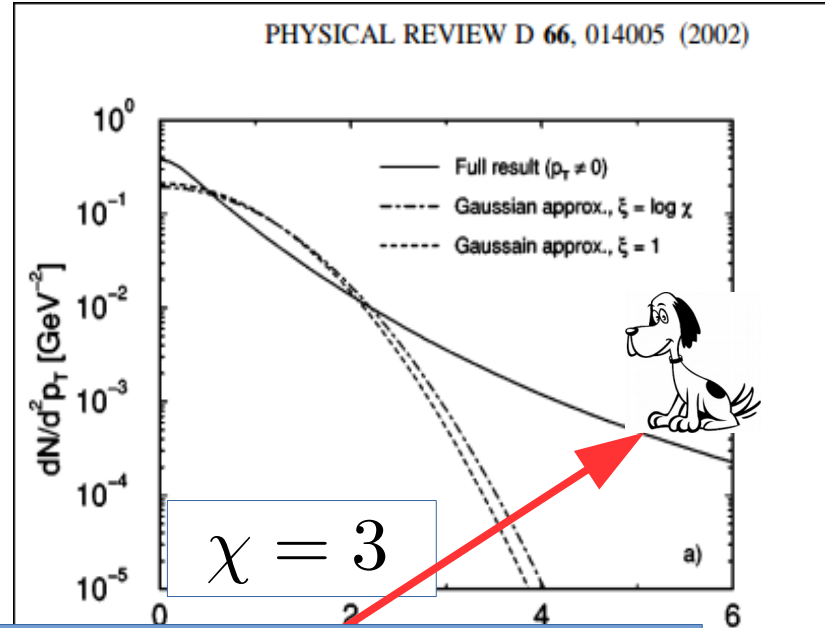
$$(\mu, \chi)$$

e.g Yukawa $\mu \approx gT$ screened parton elastic scattering

$$\frac{d\tilde{\sigma}_{el}}{d^2\mathbf{q}}(\mathbf{b}) = \int \frac{d^2\mathbf{q}}{(2\pi)^2} e^{-i\mathbf{q}\cdot\mathbf{b}} \frac{1}{\pi} \frac{\mu^2}{(\mathbf{q}^2 + \mu^2)^2} = \frac{\mu b}{4\pi^2} K_1(\mu b)$$

Mult.coll. opacity χ^n series can be summed in b-space

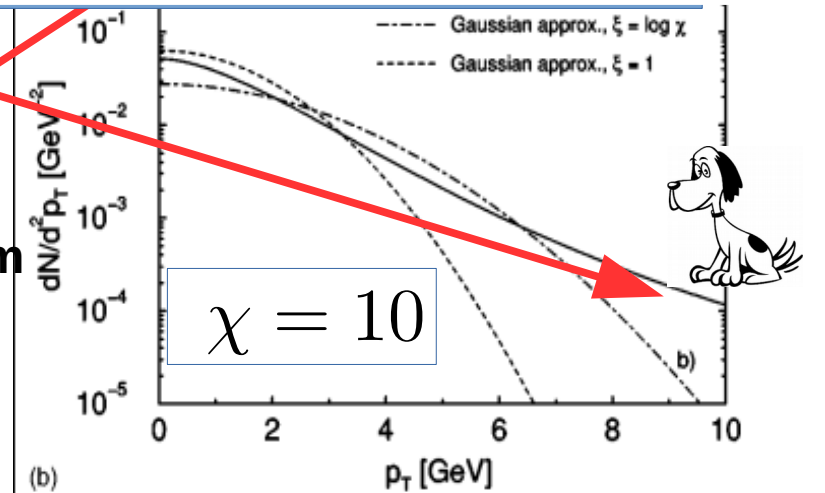
$$dN(\mathbf{p}) = e^{-\sigma_{el}T(\mathbf{b}_0)} \int d^2\mathbf{b} e^{i\mathbf{p}\cdot\mathbf{b}} e^{\tilde{\sigma}_{el}(\mathbf{b})T(\mathbf{b}_0)} dN^{(0)}(\mathbf{b})$$



$$\chi = \langle L/\lambda \rangle = \int d\mathbf{z} \rho(\mathbf{z}, \mathbf{b}_0) \int d^2\mathbf{q} \{d\sigma_{el}(\mathbf{T}(\mathbf{z}))/d^2\mathbf{q}\} \sim O(\alpha T L)$$

$$dN(\mathbf{p} \gg \chi\mu^2\xi) \approx (\chi\mu^2\xi)/\mathbf{p}^4$$

Landau tail



In large $\chi \gg 1$ lim, distrib. approaches MoliereGaus form

$$dN(\mathbf{p}) = \int d^2\mathbf{b} e^{i\mathbf{p}\cdot\mathbf{b}} \frac{1}{(2\pi)^2} \frac{e^{-\chi\mu^2\xi b^2/2}}{\chi\mu^2\xi} = \frac{1}{2\pi} \frac{e^{-p^2/2\chi\mu^2\xi}}{\chi\mu^2\xi}$$

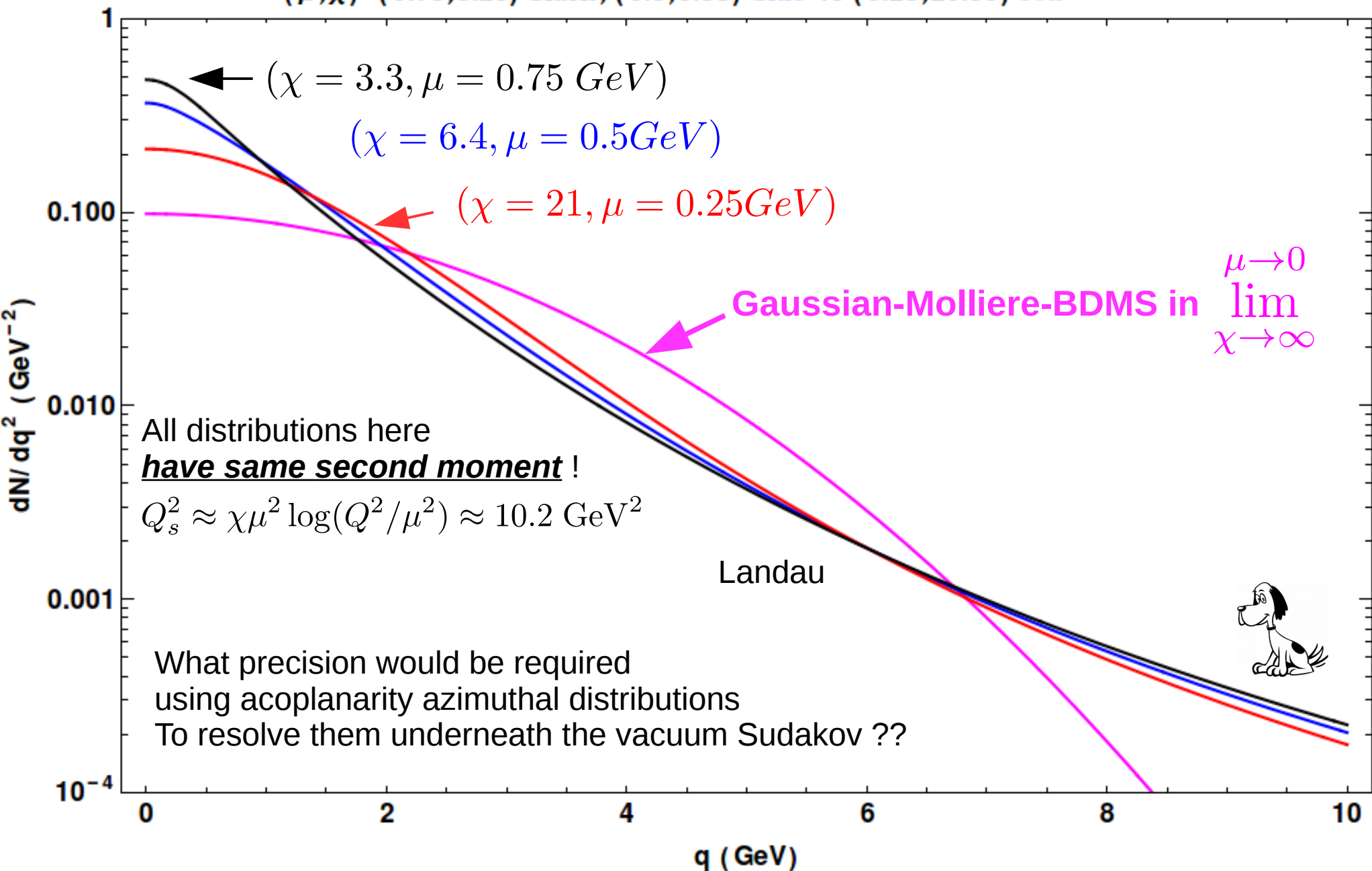
In BDMS approx this Gaussian form depends on only one "saturation scale"

$$Q_s^2 = \chi\mu^2\xi = \int dt \hat{q}(t)$$

FIG. 3. The final parton p_T distribution is shown versus p_T for two different opacities $\chi=3$ (a) and $\chi=10$ (b). We compare the full result (without the delta function contribution at $p_T \sim 0$) to the Moliere Gaussian approximation with $\xi=1$ and $\xi=\log \chi$. In this example we use $\mu^2=0.25 \text{ GeV}^2$.

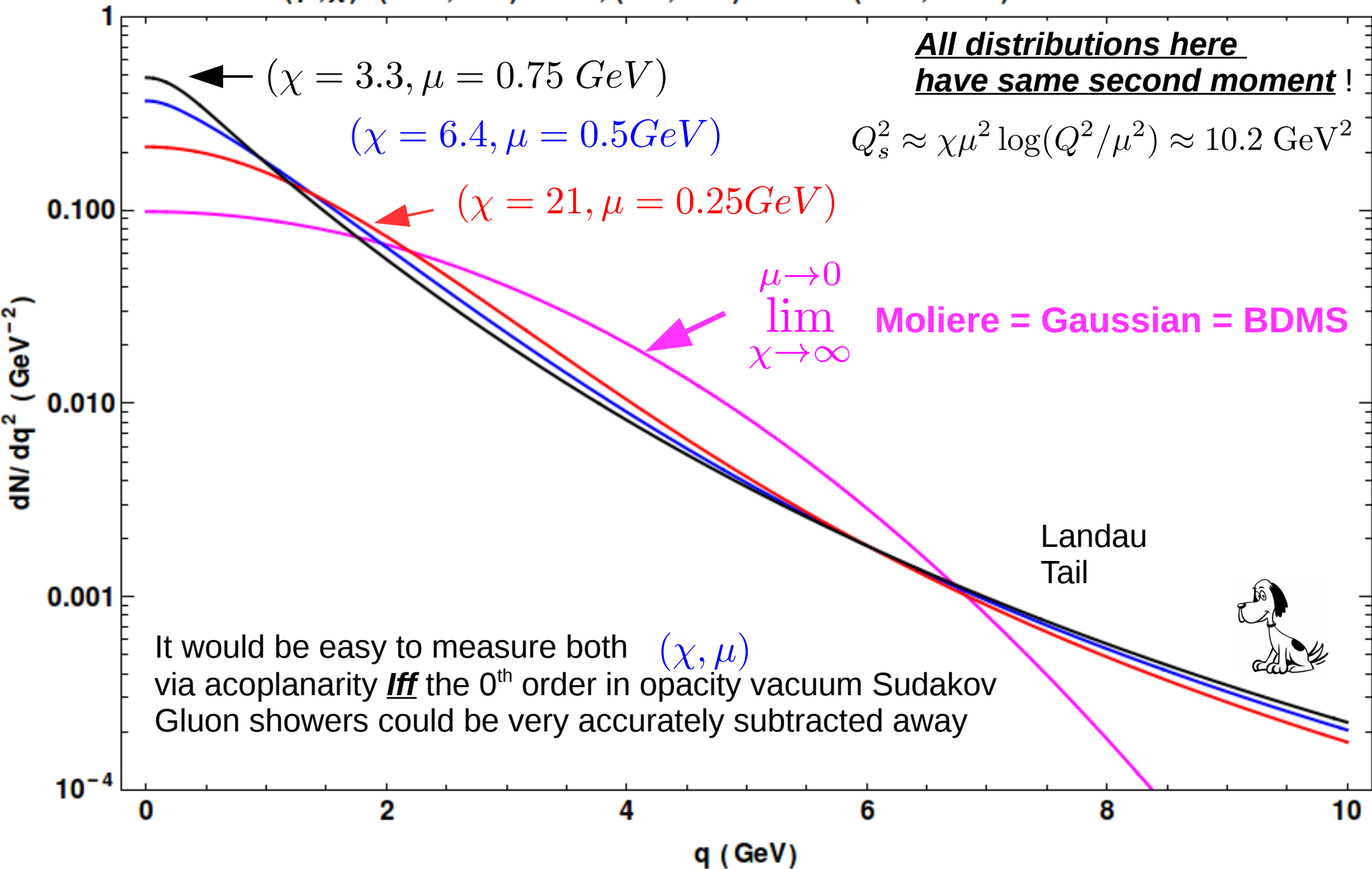
$Q=20 \text{ dN/dq}^2$ Gauss(Q_s) (magenta) vs GLV(μ, χ) shapes for fixed $Q_s^2 = 10.19$

$(\mu, \chi) = (0.75, 3.25)$ black, $(0.5, 6.38)$ blue vs $(0.25, 20.99)$ red

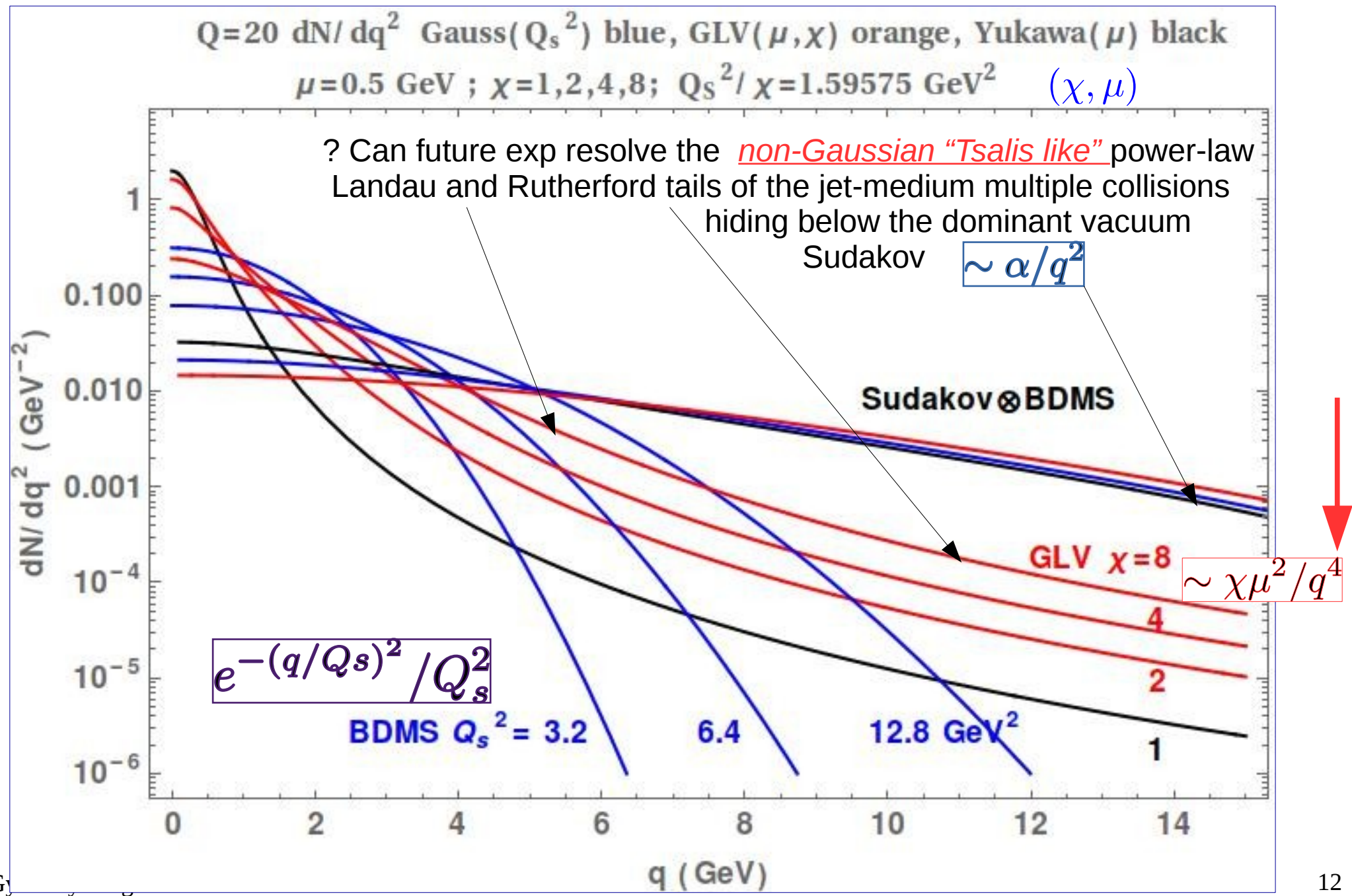


The BDMS distribution shape is very far from GLV for physical $(\chi < 20, \mu > 0.2 \text{ GeV})$

$Q=20 \text{ dN/dq}^2 \text{ Gauss}(Q_s)$ (magenta) vs GLV(μ, χ) shapes for fixed $Q_s^2 = 10.19$
 (μ, χ)=(0.75,3.25) black, (0.5,6.38) blue vs (0.25,20.99) red



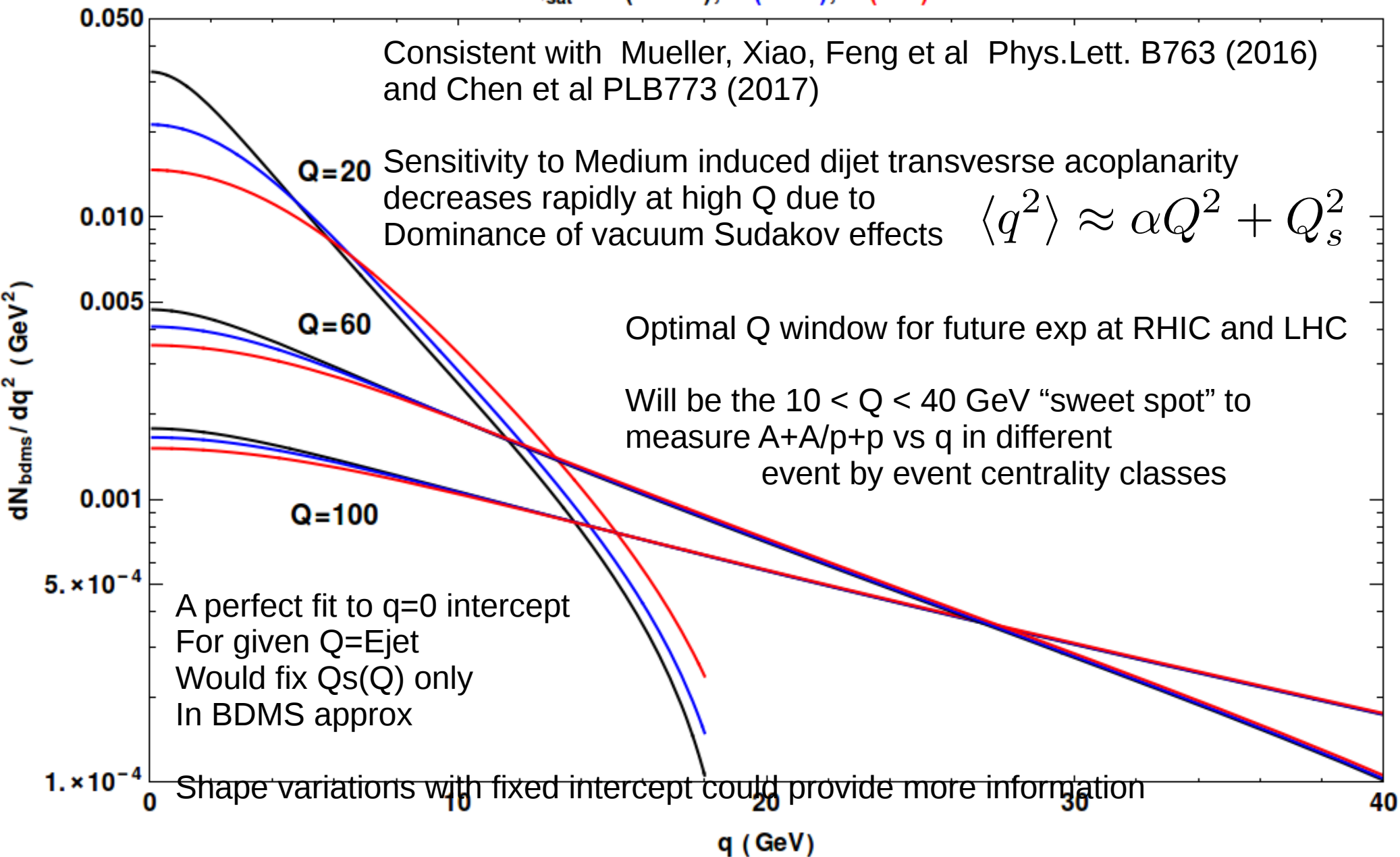
10% Percent level precision needed even to resolve BDMS Q_s from Sudakov $\sim \alpha/q^2$



One parameter, Q_s , BDMS medium convoluted with Sudakov dijet transverse distributions

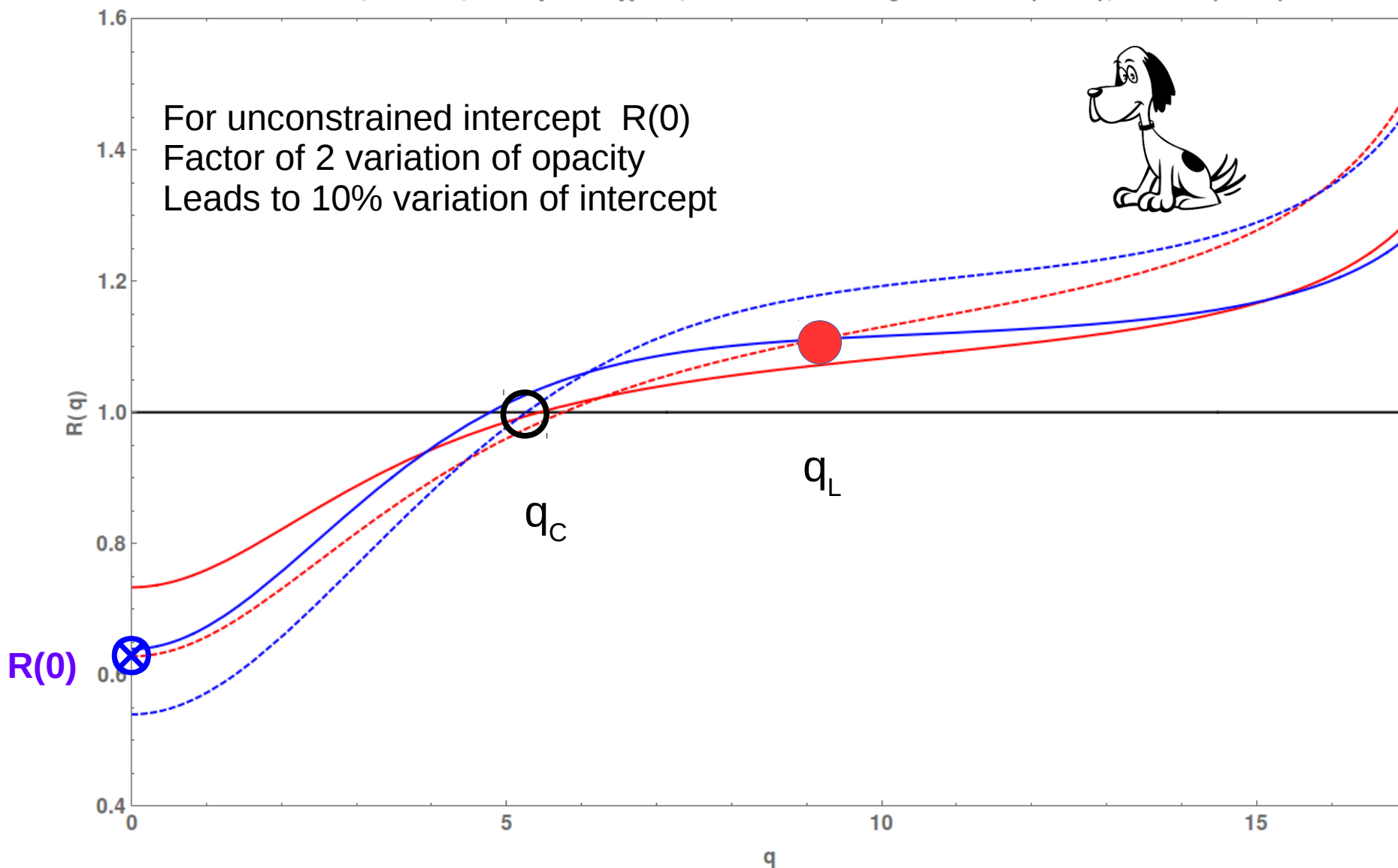
Hadron-Jet Vac ⊗ BDMS dN_{bdms}/dq^2 vs q for $Q=20, 60, 100$ GeV

$Q_{sat} = 0$ (black), 3 (blue), 5 (red) GeV

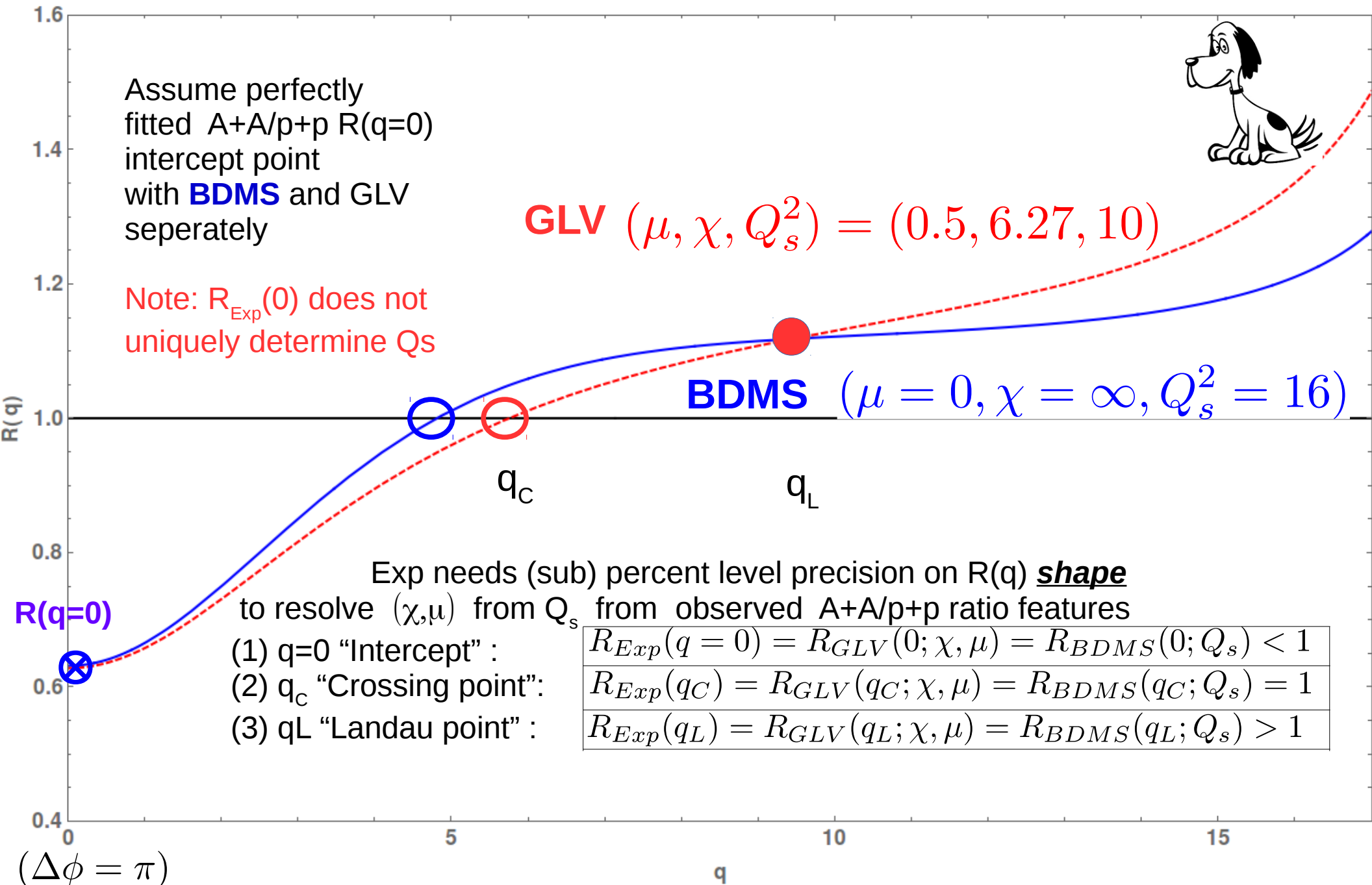


For realistic Sudakov fits to p+p need lower $\alpha \approx 0.09$ and next to leading corr.
 Requires very high precision to resolve GLV finite (χ, μ) from BDMS(Qs) medium effects

Ratio $dN(\text{Vac}+\text{GLV})/dN(\text{Vac})$ (red) vs $dN(\text{Vac}+\text{BDMS})/dN(\text{Vac})$ (blue) vs q
 for $Q=20, \alpha=0.09, \text{GLV } \mu=0.5 \chi=6, 10 \iff \text{BDMS } Q_s^2=9.57449$ (solid), 15.9575 (dash)



Ratio $dN(\text{Vac}+\text{GLV})/dN(\text{Vac})$ (red) vs $dN(\text{Vac}+\text{BDMS})/dN(\text{Vac})$ (blue) vs q



Ratio $dN(\text{Vac}+\text{GLV})/dN(\text{Vac})$ $Q_s^2=9.6$ (red), 16 (blue) vs q

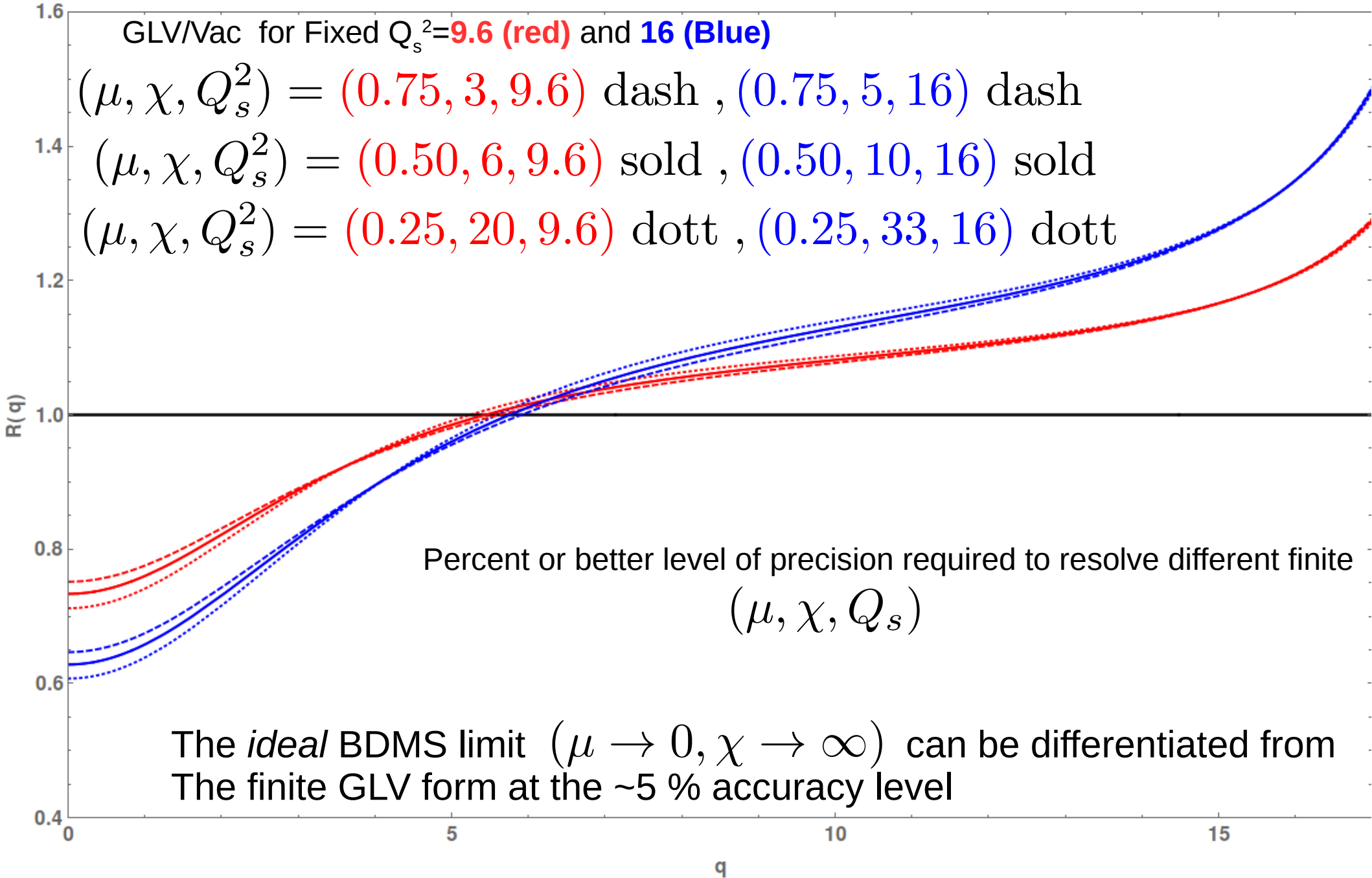
for $Q=20$, $\alpha=0.09$, $(\mu, \chi)=(0.5, 6 \& 10)$ sol, $(0.75, 3.1 \& 5.1)$ dash, $(0.25, 20 \& 33)$ dot

GLV/Vac for Fixed $Q_s^2=9.6$ (red) and 16 (Blue)

$(\mu, \chi, Q_s^2) = (0.75, 3, 9.6)$ dash, $(0.75, 5, 16)$ dash

$(\mu, \chi, Q_s^2) = (0.50, 6, 9.6)$ sold, $(0.50, 10, 16)$ sold

$(\mu, \chi, Q_s^2) = (0.25, 20, 9.6)$ dott, $(0.25, 33, 16)$ dott



Percent or better level of precision required to resolve different finite (μ, χ, Q_s)

The *ideal* BDMS limit $(\mu \rightarrow 0, \chi \rightarrow \infty)$ can be differentiated from The finite GLV form at the $\sim 5\%$ accuracy level

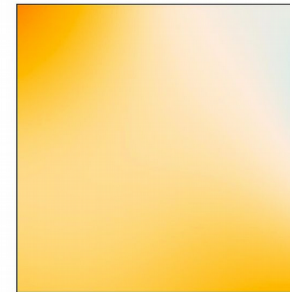
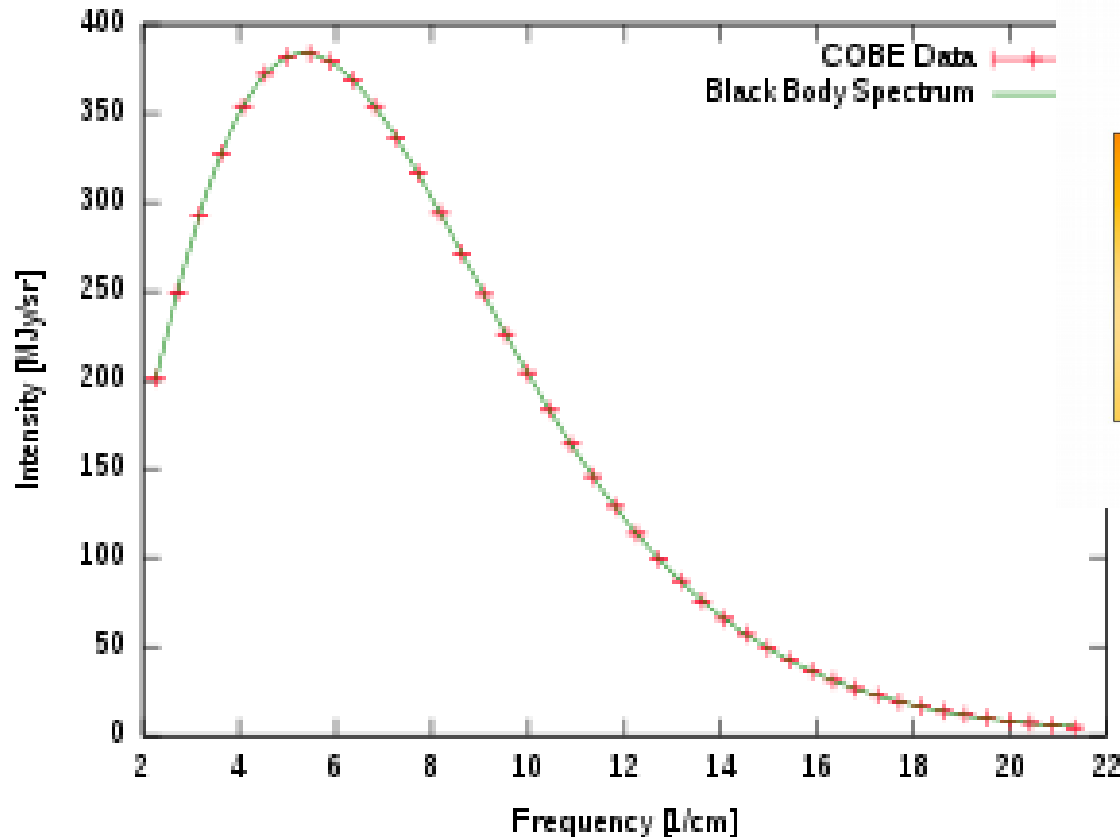
Cosmic Inspiration for pushing toward a future high precision era of A+A

1 part per 100,000 fluctuations can and have been observed to constrain cosmological models

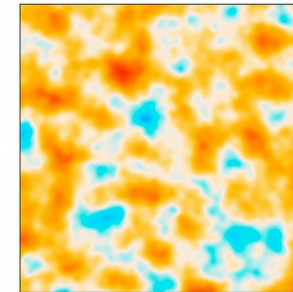
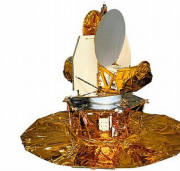
https://en.wikipedia.org/wiki/Cosmic_microwave_background

Graph of cosmic microwave background spectrum measured by the FIRAS instrument on the COBE, the most precisely measured black body spectrum in nature.[7]
The error bars are too small to be seen even in an enlarged image, and it is impossible to distinguish the observed data from the theoretical curve.

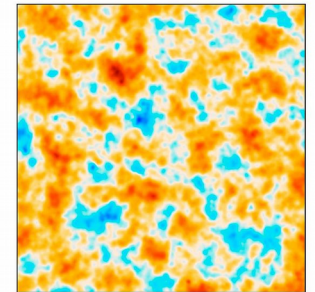
Cosmic Microwave Background Spectrum from COBE



COBE

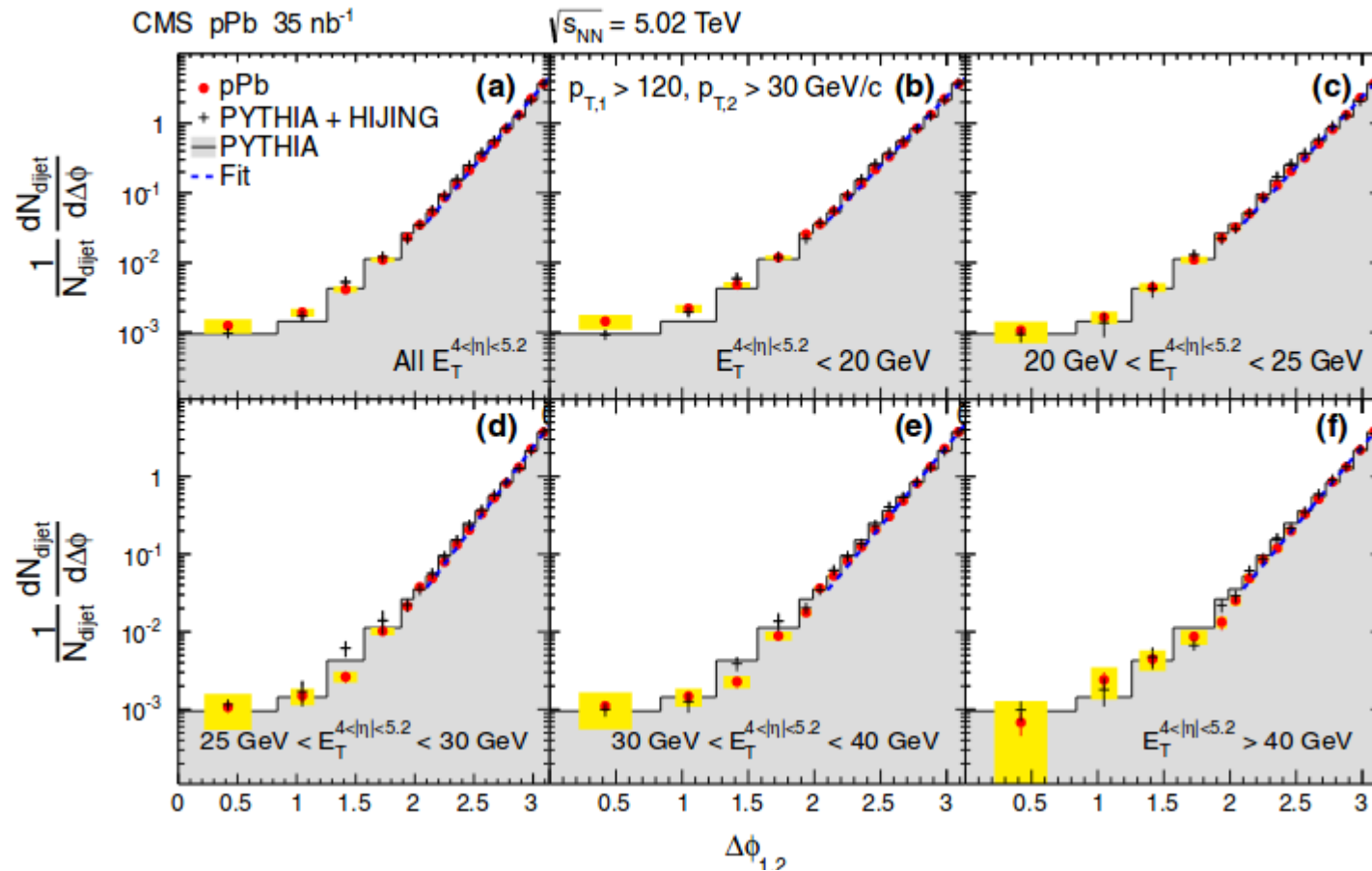


WMAP



Planck

CMS Studies of dijet transverse momentum balance and pseudorapidity distributions in pPb collisions at 5.02 TeV have already achieved great precision



Very high precision has (after 30 years) been reached at LHC in pp and pA that constrain vacuum Sudakov acoplanarity due to jet gluon showers. Thus Sudakov A, B and *non-perturb* D factors can now be tuned to high accuracy and to higher NN..LO α_s^n

Multiple jets and γ -jet correlation in high-energy heavy-ion collisions

Luo, Cao, He, Wang CCNU
arXiv:1803.06785 [hep-ph]

High $p_T \sim 100$ GeV makes small angle deviations from π nearly independent of medium effect and are dominated by vacuum Sudakov effects.

At large angles < 2 there is a predicted suppression of gam-jet correlations due to multiple induced jet suppression complementary to RAA(p_T) Sensitive to $q_{\text{hat}}(E, T)$.

“Dominance of the Sudakov form factor in γ -jet correlation from soft gluon radiation in large p_T hard processes pose a challenge for using γ -jet azimuthal correlation to study medium properties via large angle parton-medium interaction.”

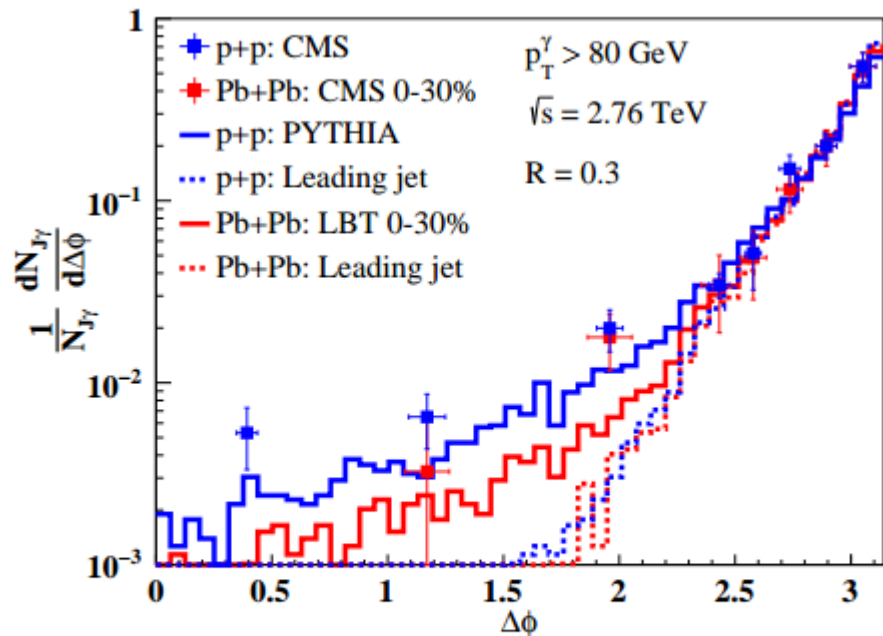


FIG. 6: (Color online) Angular distribution of γ -jet in central (0–30%) Pb+Pb (red) and p+p collisions (blue) at $\sqrt{s} = 2.76$

Exp should focus in “sweet spot”

$$2.4 < \Delta\phi < \pi$$

To reduce large distortion due to the quenching of multiple medium minijets unrelated to the dijet

High precision needed to map out the temperature and jet energy dependence of

the microscopic composition and rates

$$\Gamma_{ab}(q_{\perp}, T) = \rho_b(T) d^2 \sigma_{ab}(T) / d^2 q_{\perp}$$

Will need “multi-messenger” precision experimental constraints to get beyond simple Qs phenomenology and try to deconvolute Γ_{ab} from soft+jet and soft+dijet observables
These rates have so far been hidden inside

$$Q_s^2(a) \equiv \left\langle q_{\perp}^2 \frac{L}{\lambda} \right\rangle_a \equiv \int dt \sum_b \hat{q}_{ab}(x(t), t) \equiv \sum_b \int dt d^2 q_{\perp} q_{\perp}^2 \Gamma_{ab}(q_{\perp}, t)$$

Qs is a path integral functional over ensemble averaged over evolving e-by-e fluctuating local temperature and flow velocity fields $T(x,t)$, $u(x,t)$ and limited to the second moment in qT space

From our extensive global CIBJET=ebe IC + VISHNU + CUJET3.1
Analysis of RHIC+LHC1+LHC2 data on light and heavy single jet RAA & vn
There is strong indication for highly nontrivial nonperturbative physics near T_c
That can be captured by the semi-Quark+Gluon+Monopole Plasma model
Of the QCD perfect fluid consistent not only with Exp data but also Lattice QCD data
As well as providing a microscopic picture of how near unitarity bound eta/s can arise
Through emergent color magnetic monopole d.o.f. in the cross over temperature range

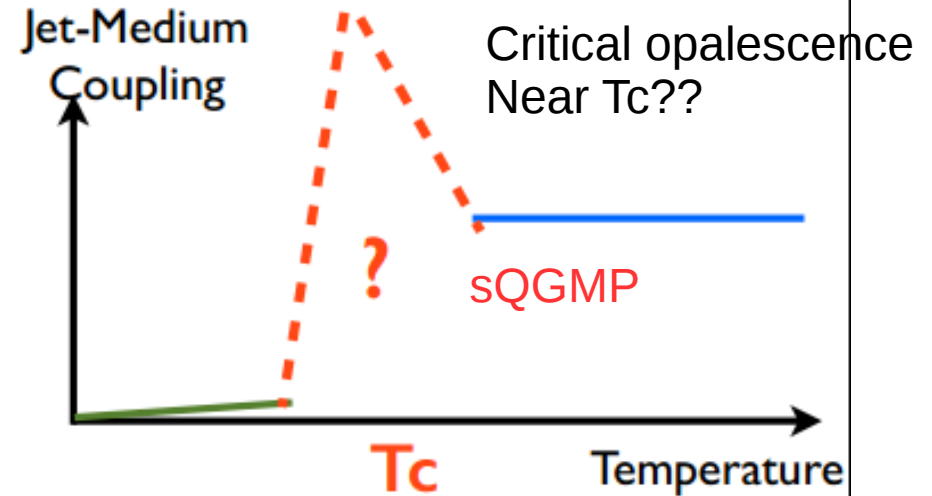
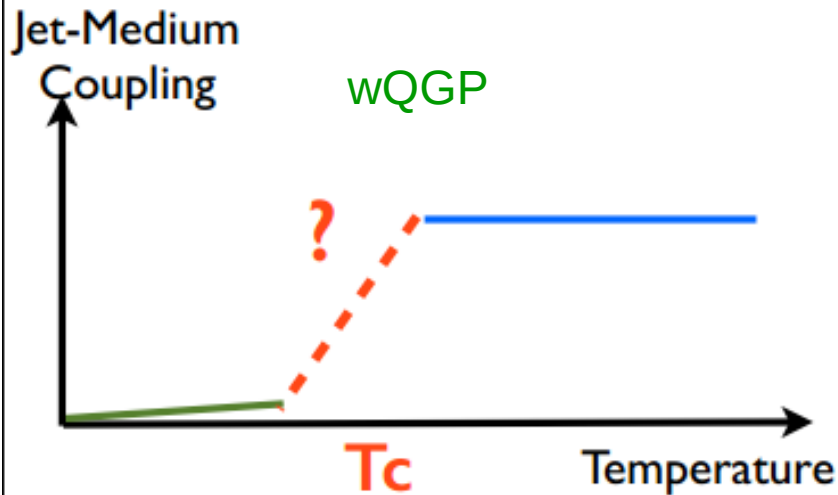
Precision acoplanarity *distribution shapes can test such models* on the color d.o.f in the near Perfect QCD fluids by constraining the microscopic differential scattering rates, Γ_{ab} , near $T \sim T_c$?

Monopole component near T_c
could account for near perfect fluidity

$$\frac{d\sigma_{EM}}{dq_{\perp}^2} \sim \frac{\alpha_E \alpha_M}{q_{\perp}^4} \sim \frac{1}{\alpha_E^2} \frac{d\sigma_{EE}}{dq_{\perp}^2} \gg \frac{d\sigma_{EE}}{dq_{\perp}^2}$$

J.Liao 2015

From “Transparency” to Opaqueness



**The temperature dependence of jet-medium coupling
has profound consequences!**

J.Liao 2015

CIBJET was developed by A. Buzzatti, J.Xu, and Shuzhe Shi to quantitatively test this

idea with global χ^2 analysis of SPS, RHIC and LHC RAA, v_2 , v_3 data

$$\begin{aligned}
 \hat{q}_F(E, T) = & \int_0^{6ET} dq_{\perp}^2 \frac{2\pi}{(\mathbf{q}_{\perp}^2 + f_E^2 \mu^2(\mathbf{z}))(\mathbf{q}_{\perp}^2 + f_M^2 \mu^2(\mathbf{z}))} \rho(T) \\
 & \times \left\{ [C_{qq}f_q + C_{qg}f_g] \cdot [\alpha_s^2(\mathbf{q}_{\perp}^2)] \cdot [f_E^2 \mathbf{q}_{\perp}^2 + f_E^2 f_M^2 \mu^2(\mathbf{z})] + \right. \\
 & \left. [C_{qm}(1 - f_q - f_g)] \cdot [1] \cdot [f_M^2 \mathbf{q}_{\perp}^2 + f_E^2 f_M^2 \mu^2(\mathbf{z})] \right\}, \quad (14)
 \end{aligned}$$

$$\begin{aligned}
 \hat{q}_g(E, T) = & \int_0^{6ET} dq_{\perp}^2 \frac{2\pi}{(\mathbf{q}_{\perp}^2 + f_E^2 \mu^2(\mathbf{z}))(\mathbf{q}_{\perp}^2 + f_M^2 \mu^2(\mathbf{z}))} \rho(T) \\
 & \times \left\{ [C_{gq}f_q + C_{gg}f_g] \cdot [\alpha_s^2(\mathbf{q}_{\perp}^2)] \cdot [f_E^2 \mathbf{q}_{\perp}^2 + f_E^2 f_M^2 \mu^2(\mathbf{z})] + \right. \\
 & \left. [C_{gm}(1 - f_q - f_g)] \cdot [1] \cdot [f_M^2 \mathbf{q}_{\perp}^2 + f_E^2 f_M^2 \mu^2(\mathbf{z})] \right\}, \quad (15)
 \end{aligned}$$

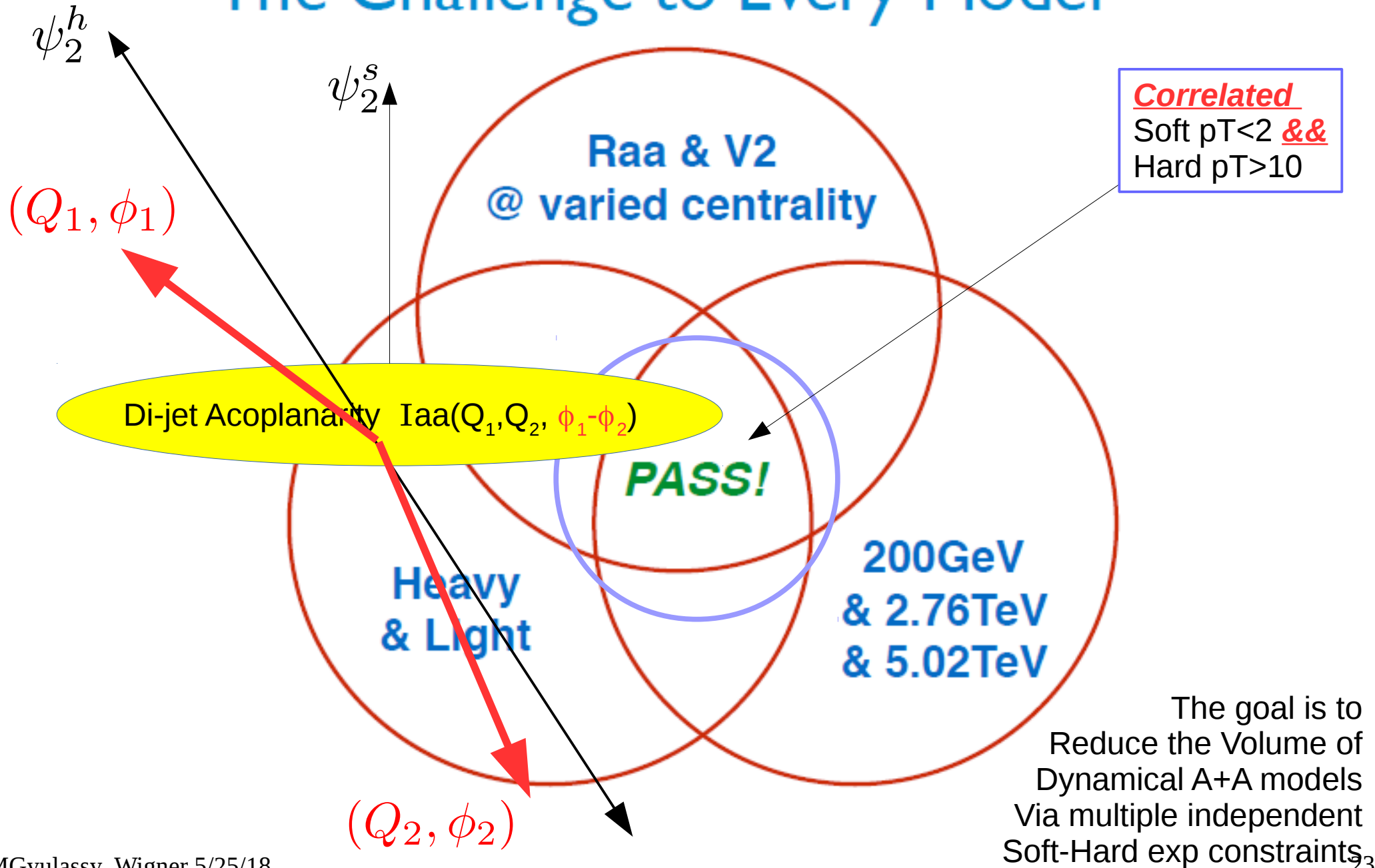
$$\begin{aligned}
 \hat{q}_m(E, T) = & \int_0^{6ET} dq_{\perp}^2 \frac{2\pi}{(\mathbf{q}_{\perp}^2 + f_E^2 \mu^2(\mathbf{z}))(\mathbf{q}_{\perp}^2 + f_M^2 \mu^2(\mathbf{z}))} \rho(T) \\
 & \times \left\{ [C_{mq}f_q + C_{mg}f_g] \cdot [1] \cdot [f_E^2 \mathbf{q}_{\perp}^2 + f_E^2 f_M^2 \mu^2(\mathbf{z})] + \right. \\
 & \left. [C_{mm}(1 - f_q - f_g)] \cdot [\alpha_s^{-2}(\mathbf{q}_{\perp}^2)] \cdot [f_M^2 \mathbf{q}_{\perp}^2 + f_E^2 f_M^2 \mu^2(\mathbf{z})] \right\}. \quad (16)
 \end{aligned}$$

The HTL wQGP model of the perfect QCD fluid is obtained with $f_E=1$ and $f_M=0$ AND setting poly loop $L=1$ AND chiral suscept =1. Global χ^2 rules out this models

And internally it is inconsistent with η/s near $1/4\pi$ and hence inconsistent with soft observables

Conclusion: we need to add dijet acoplanarity and strive for higher precision
 Demanding every model to pass all global soft+hard probes tests consistently
 In order to extract conclusions about the novel color structure of QCD perfect fluids

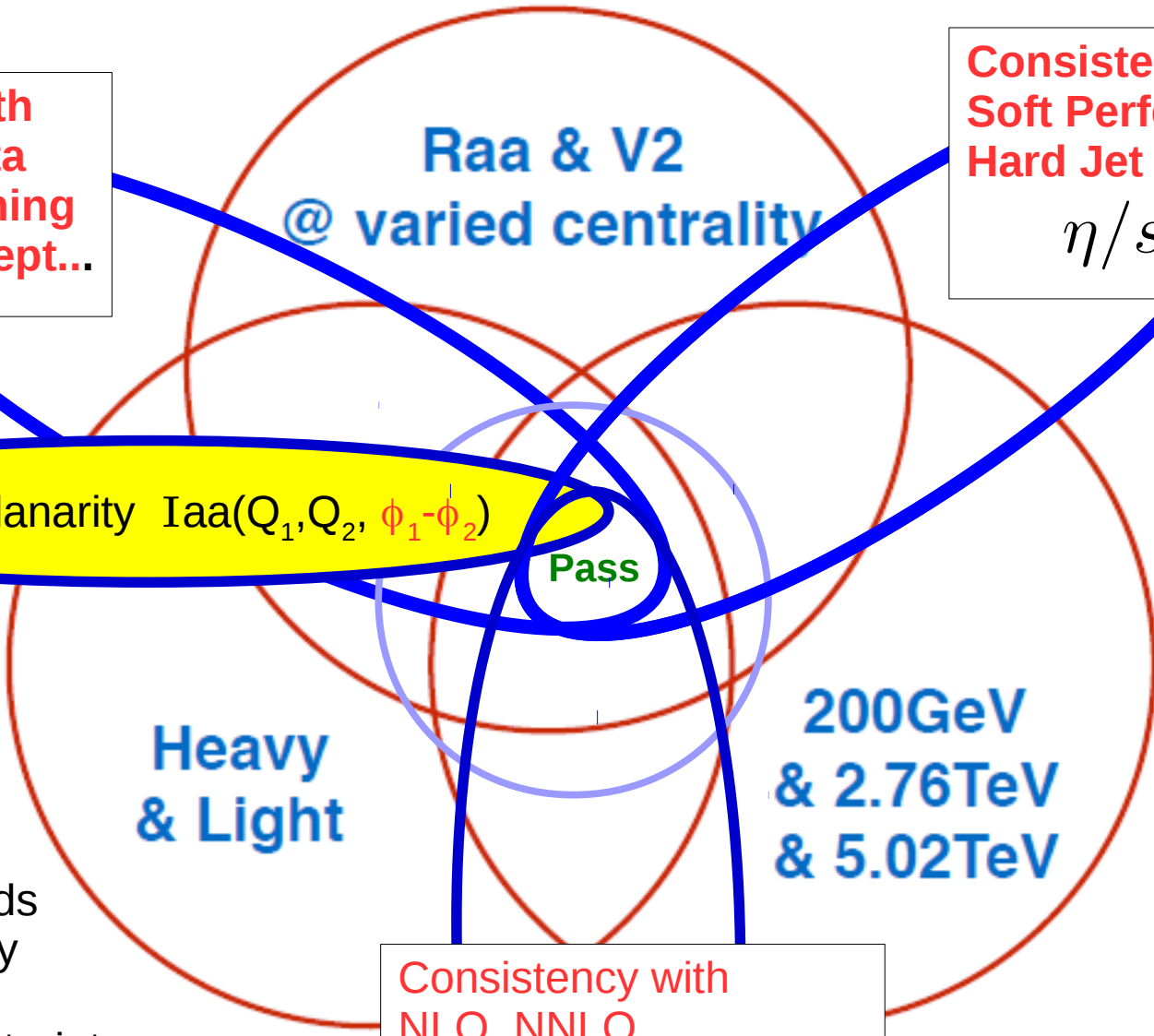
The Challenge to Every Model



The Challenge to Every Model

Consistency with Lattice QCD data On EOS, Screening Polyakov, Suscept...

Consistency between Soft Perfect Fluidity and Hard Jet Quenching η/s vs s/\hat{q}



Consistency with NLO, NNLO... Vacuum Jet Sudakov and hard pQCD physics

Steps needed towards Reducing the entropy of A+B modeling via Theo & Exp constraints

Appendix: Review of past and current advances with CUJET and CIBJET

Jiechen Xu , J.Liao, MG, Chin.Phys.Lett. 32 (2015), JHEP 1602 (2016) 169

Shuzhe Shi, J.Xu, J.Liao, MG, QM17, NPA967 (2017) 648-651

Shuzhe Shi, J.Liao, MG: arXiv:1804.01915

The Liao-Shuryak sQGMP Transition Phase

$T \ll \Lambda_{\text{QCD}}$

$T \sim \Lambda_{\text{QCD}}$

$T \gg \Lambda_{\text{QCD}}$

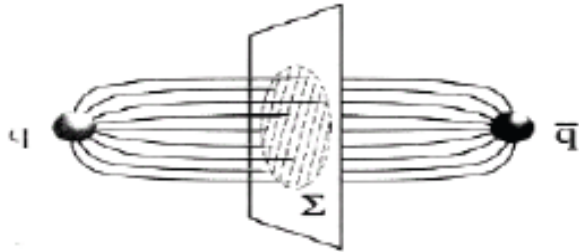
Vacuum: confined

T_c

sQGP

wQGP: screening

T



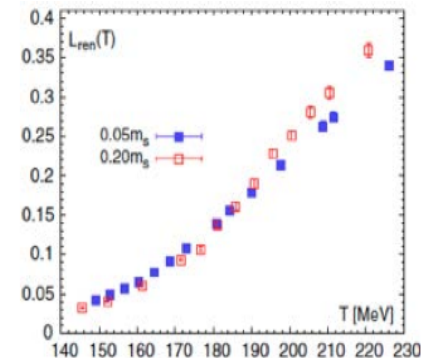
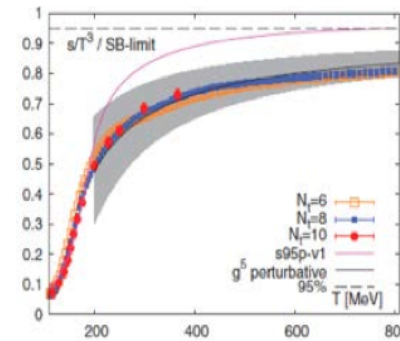
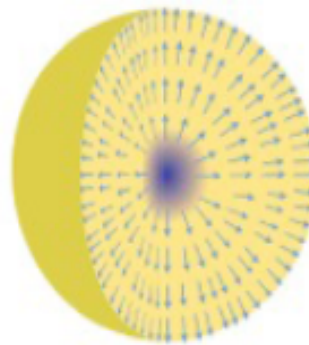
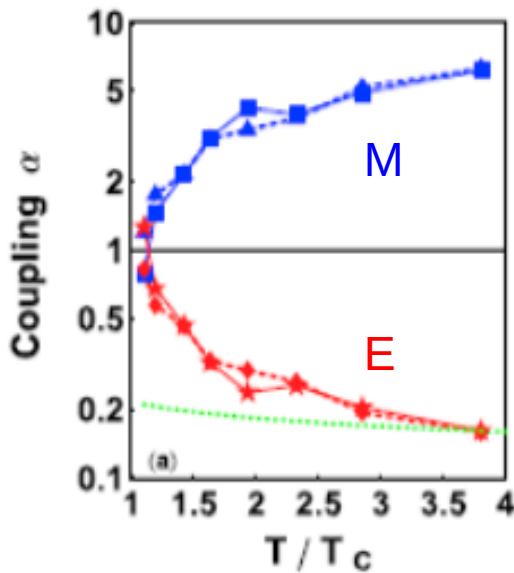
Electric Flux Tube:
Magnetic Condensate

Emergent plasma with E & M charges:
chromo-magnetic monopoles are the “missing DoF”

Plasma of E-charges
E-screening: $g T$
M-screening: $g^2 T$

$$L(\mathbf{x}) = \frac{1}{N_c} \text{tr} \mathcal{P} \exp \left[i g \int_0^{1/T} A_4(\tau, \mathbf{x}) d\tau \right]$$

$$\alpha_E * \alpha_M = 1.$$



A region around T_c with liberated degrees of freedom but only partially liberated color-electric objects—missing D.o.F.:
semi-OGP + emergent magnetic component

Jingeng Liao and Ed Shuryak

Phys.Rev.C75:054907,2007; Phys.Rev.Lett.101:162302,2008;
Phys.Rev.C77:064905,2008; Phys.Rev.D82:094007,2010;
Phys.Rev.Lett.109:152001,2012.

❖ Slide from Jinfeng Liao, APS DNP Hawaii 2014

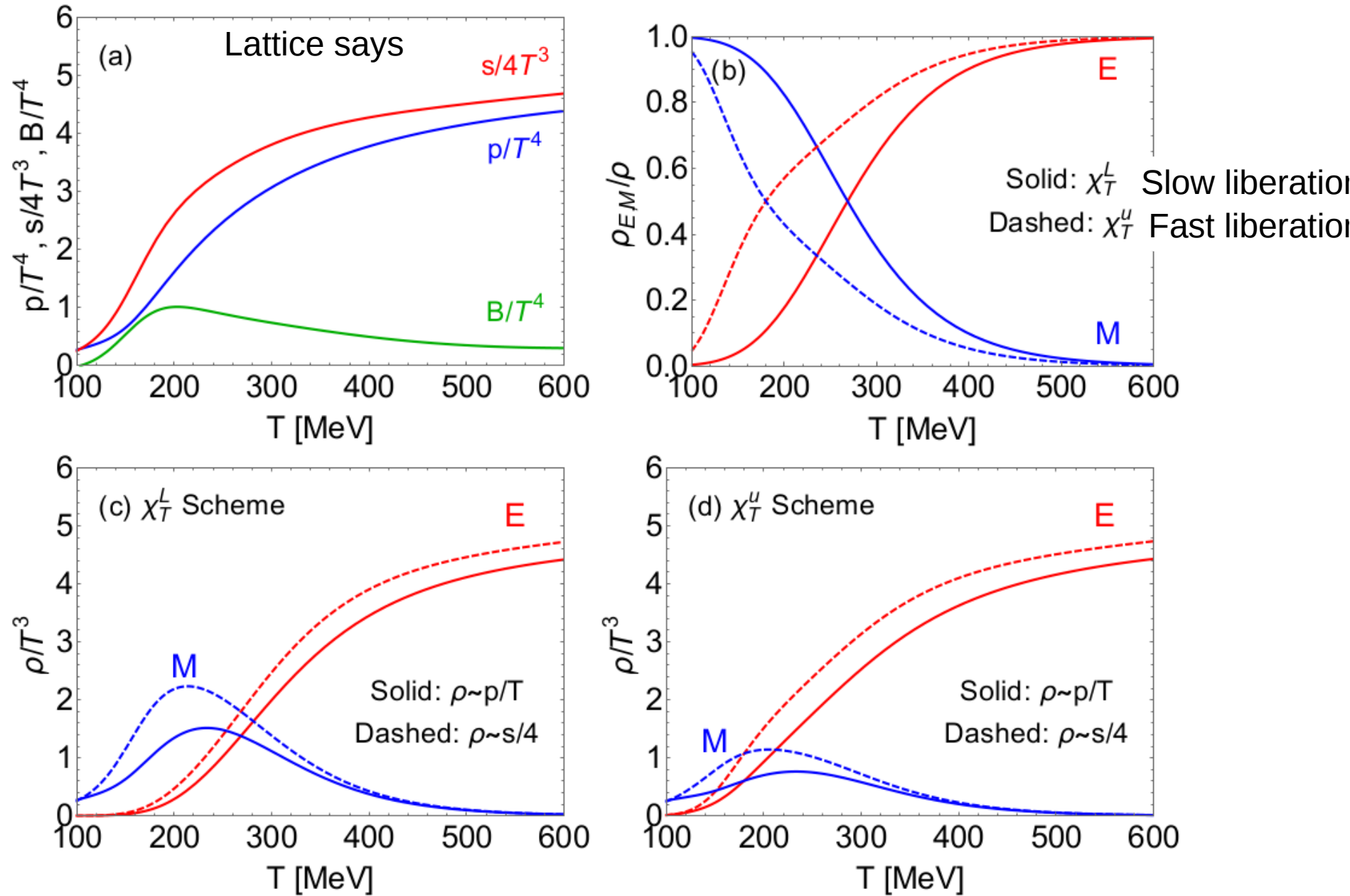
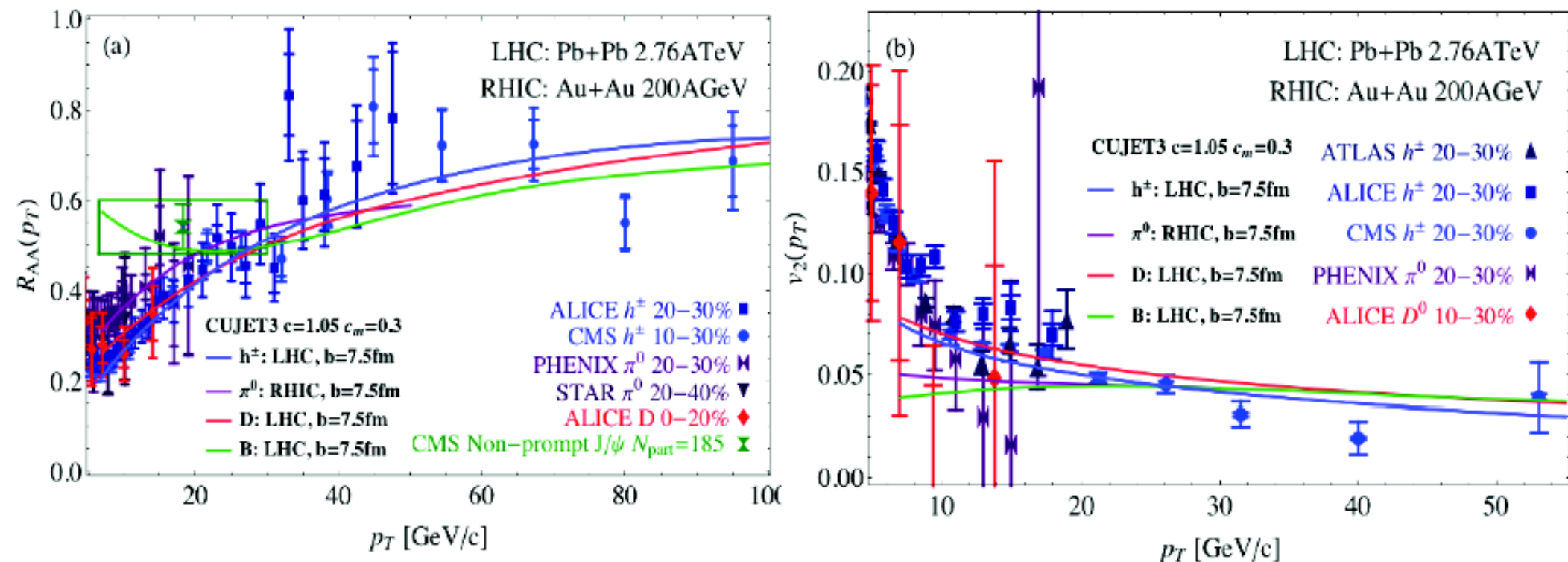


Figure 6. (Color online) (a) The effective ideal quasiparticle density, $\rho/T^3 = \xi_p P/T^4$, in the Pressure Scheme (PS, Blue) is compared with effective density, $\rho/T^3 = \xi_p S/4T^3$, in the Entropy Scheme (ES, Red) based on fits to lattice data from HotQCD Collaboration [56]. The difference is due to an interaction “bag” pressure $-B(T)/T^4$ (Green) that encodes the QCD conformal anomaly

$$\chi^2/dof \sim 1.0 - 1.3 \quad \longrightarrow \quad (\alpha_c = 0.9 \pm 0.1, c_m = 0.25 \pm 0.03)$$



J.Xu, J.Liao, MG, Chin.Phys.Lett. 32 (2015)

The combined set of observables

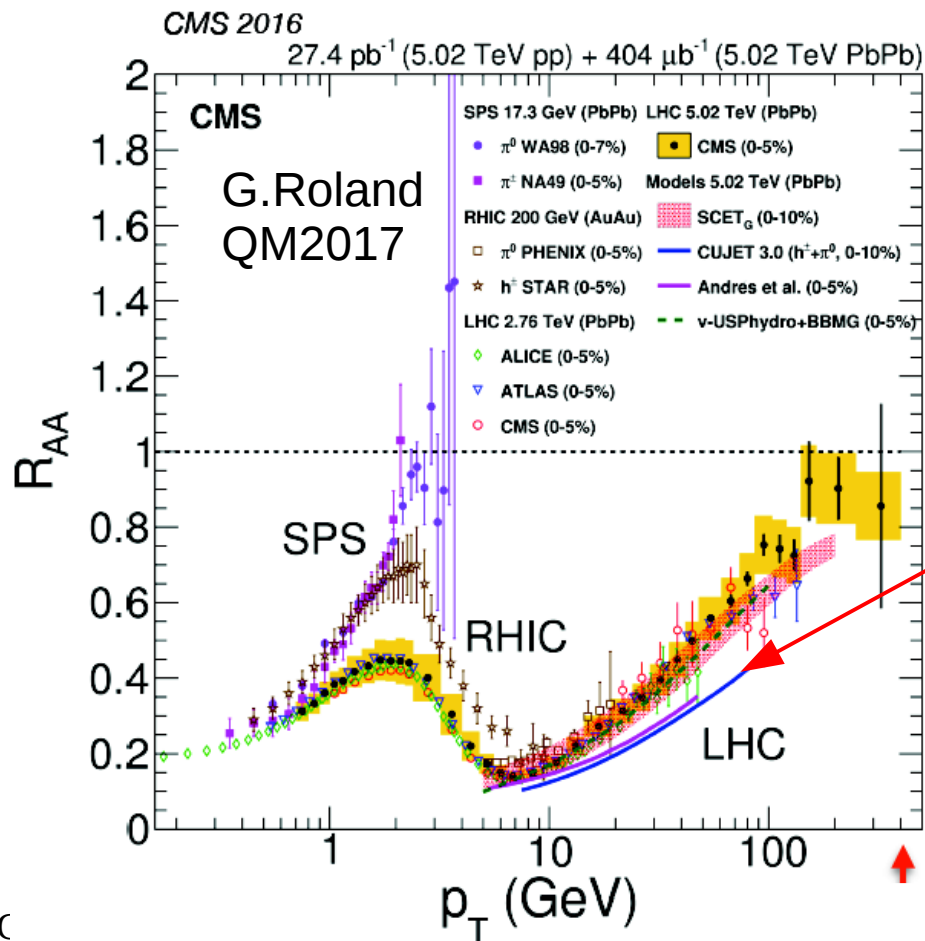
$$(R_{AA} + v_2) * (RHIC + LHC) * (\text{pion} + D + B)$$

are consistently accounted for in CUJET3.0 using lattice data constrained sQGMP near T_c + pQCD/DGLV jet quenching

At QM17 CMS/LHC2 found discrepancies with CUJET3.0 predictions for the centrality dependence of 5ATeV RAA and v_2

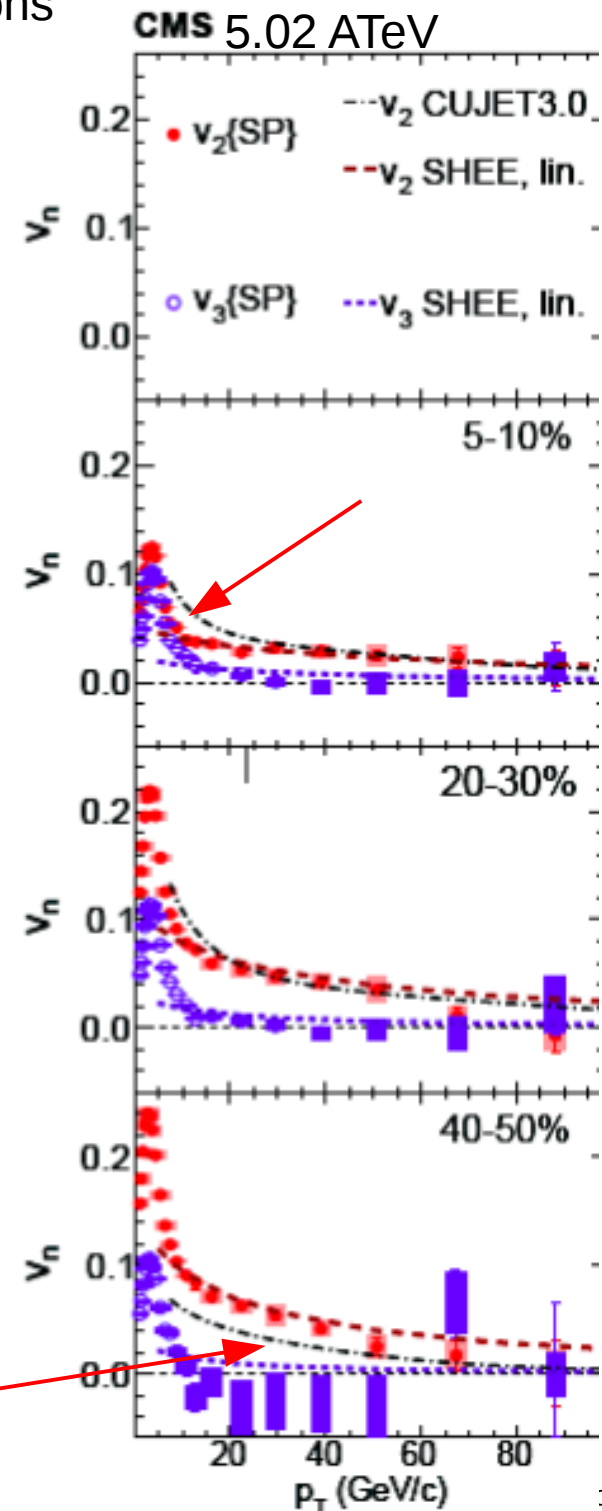
Shuzhe Shi found 3 bugs in CUJET3.0, now corrected in **CUJET3.1**

- 1) Initial parton spectra for 5.02 ATeV were erroneously read in
- 2) VISHNU hydro fluid grid for 5.02 incorrectly oriented in CUJET3.0
- 3) The parton spectra range was set too low for the 5.02 run

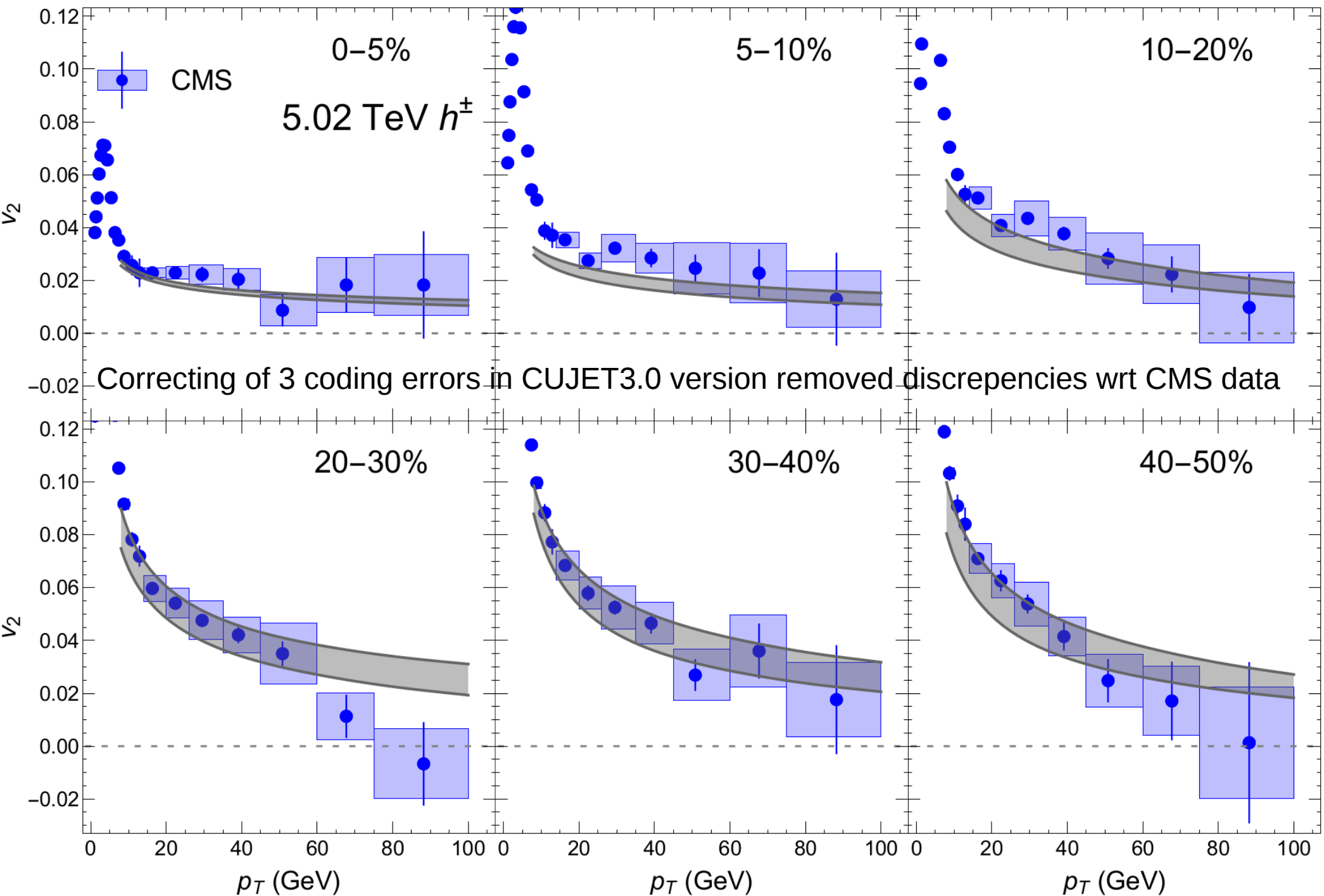


3 Bugs in CUJET3.0 led at 5TeV LHC2 to

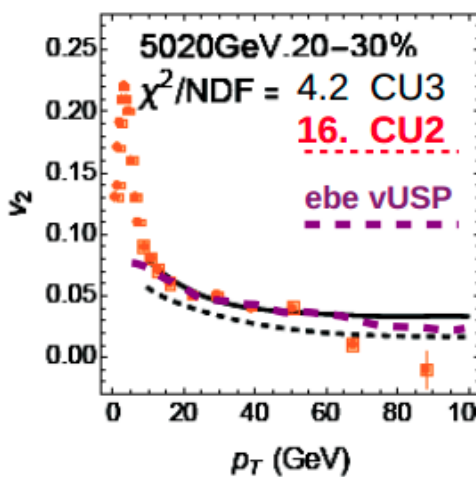
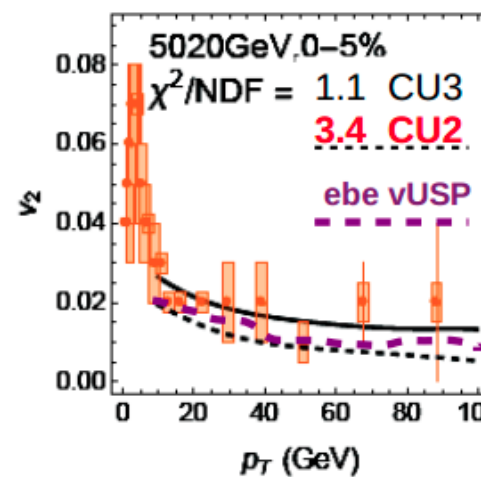
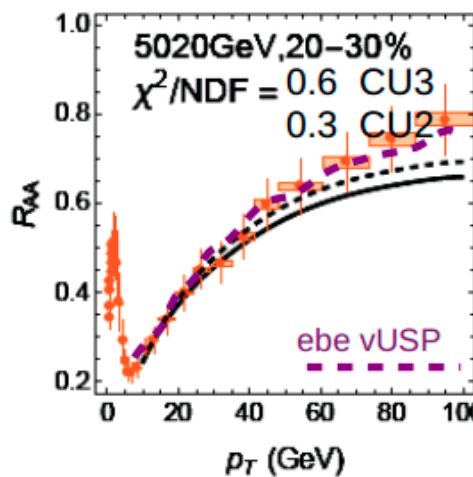
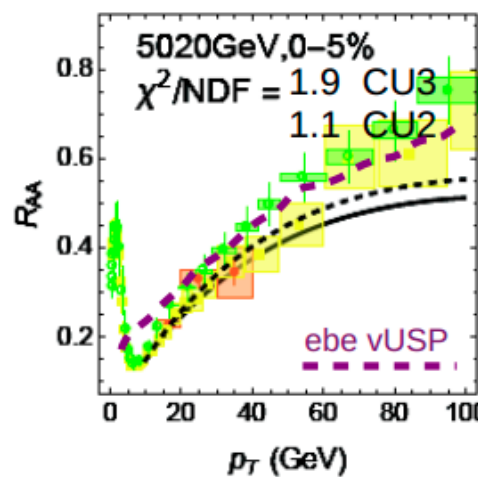
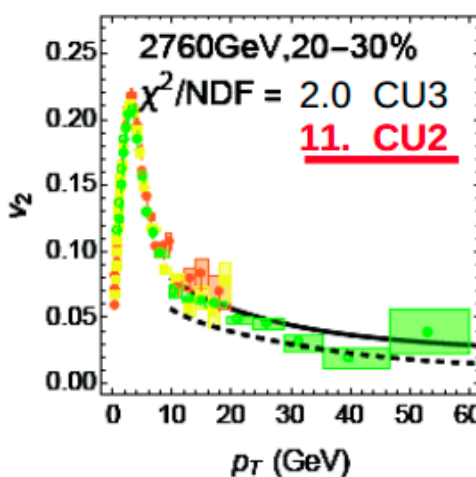
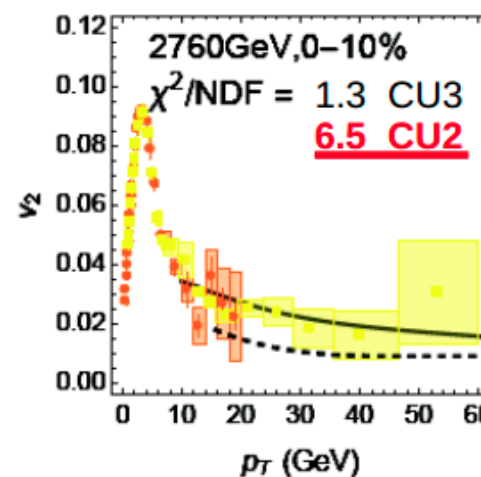
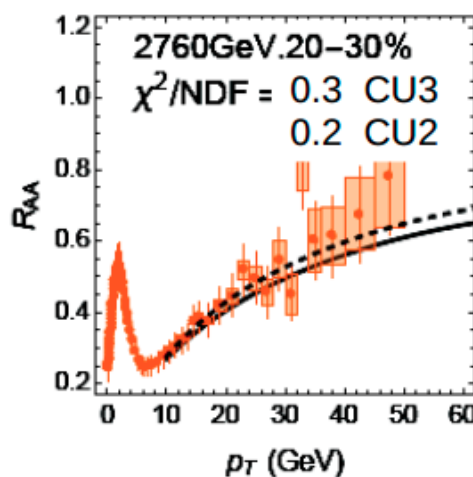
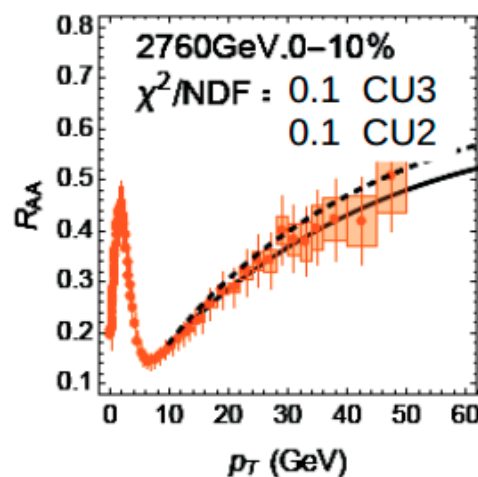
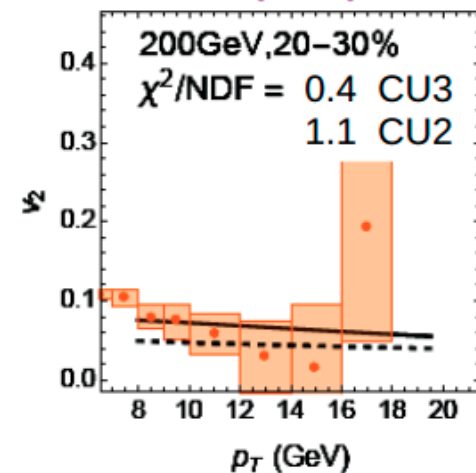
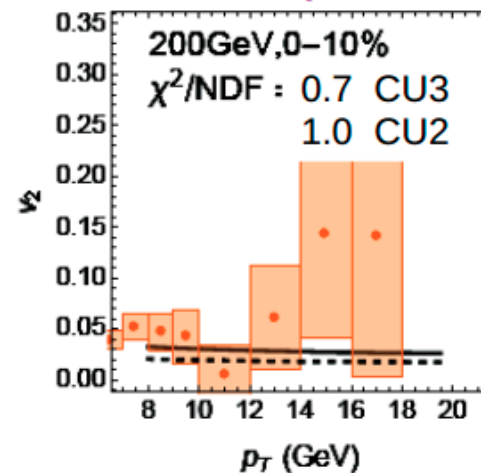
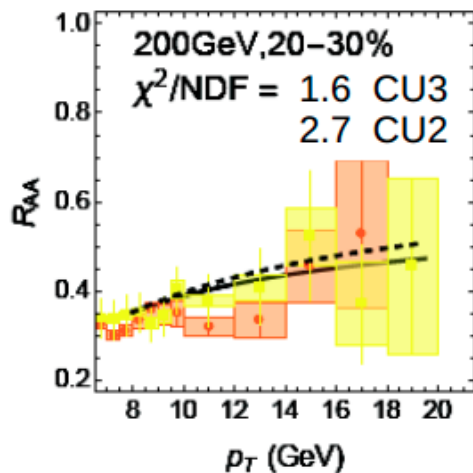
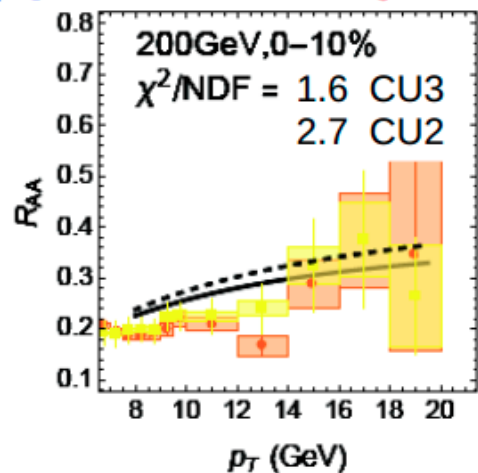
- 1) overquench RAA
- 2) predict wrong Centrality dep of v_2



(Shuzhe Shi et al 2018) CUJET3.1 test of v_2 centrality dependence at 5.02A TeV vs CMS data



pQGP/CUJET2.1 vs sQGMP/CUJET3.1 vs RHIC&LHC vs ebe/vUSP+BBMG (J.Noronha-Hostler PRC95 (2017))



Combined RHIC+LHC1+LHC2 data RAA+v2 fit $\chi^2(\alpha_c, c_m)$ surfaces

Assuming Polyakov suppressed color electric semi-q+g + monop $\chi_T^L = c_q L + c_g L^2$

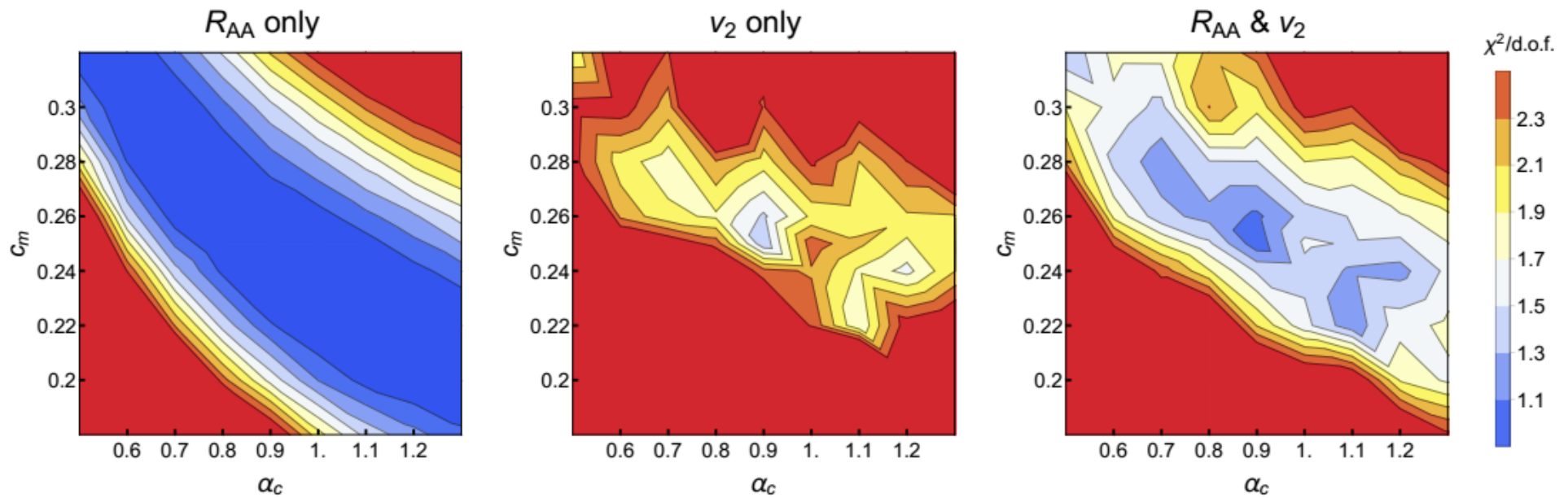
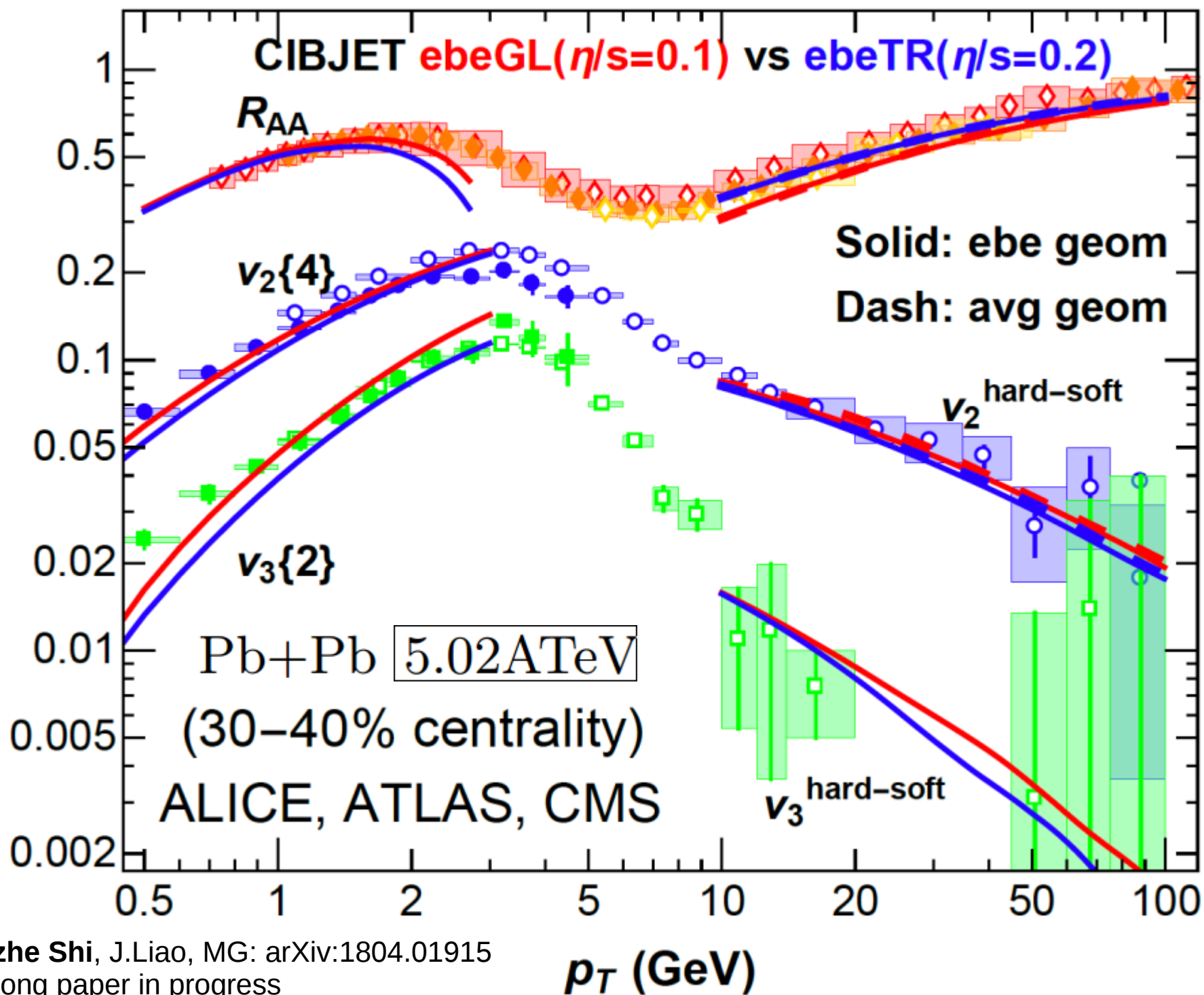


FIG. 1: (color online) $\chi^2/\text{d.o.f}$ comparing χ_T^L -scheme CUJET3 results with RHIC and LHC data. Left: $\chi^2/\text{d.o.f}$ for R_{AA} only. Middle: $\chi^2/\text{d.o.f}$ for v_2 only. Right: $\chi^2/\text{d.o.f}$ including both R_{AA} and v_2

An open question at QM 2017 was how much would the inclusion of ebe fluctuations of Initial Conditions modify CUJET3.1 results using only event averaged IC geometries. Shuzhe Shi generalized CUJET3.1 to **ebe** CIBJET = **ebe** IC+VISHNU+CUJET3.1 framework And found that with CIBJET ebe only makes $\sim 10\%$ changes relative to event ave geom

Consistent Soft-Hard Event Engineering in the ebe CIBJET framework



Shuzhe Shi, J.Liao, MG: arXiv:1804.01915
and long paper in progress

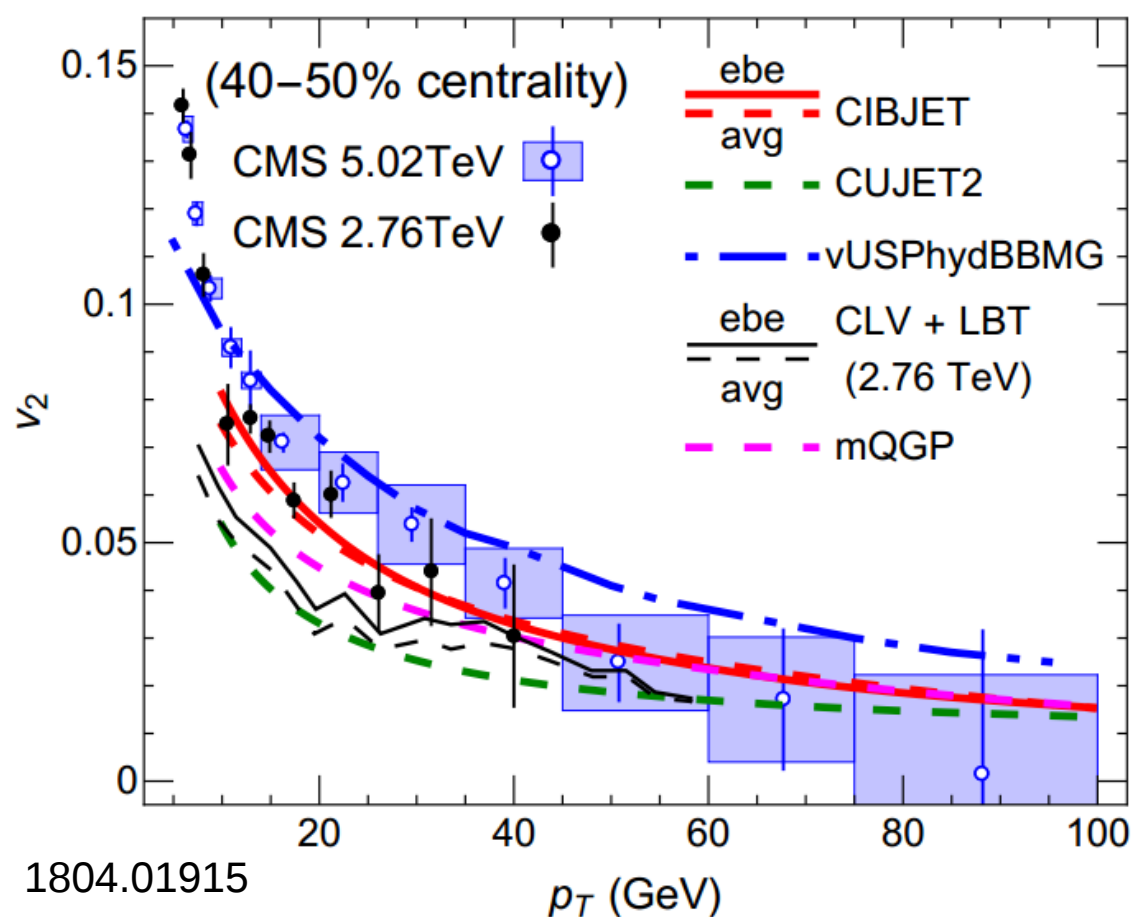


FIG. 2: (color online) A comparison of the azimuthal anisotropy coefficient $v_2(p_T)$ at high transverse momentum, computed from different models for 40-45% Pb+Pb collisions at 2.76 ATeV and 5.02 ATeV. All models are calibrated with R_{AA} data already. Both CIBJET (red) and CLV+LBT (black) [39] models demonstrate very small difference between their respective average-geometry results (dashed curves) and event-by-event (solid curves) results. Compared with available CMS measurements [37, 41], results from CIBJET model as well as event-by-event vUSPhydBBMG model [11] agree

There is Current
Tension between the
degenerate
Solutions of RAA-v2
puzzle with

Ebe CIBJET using
sQGMP rates

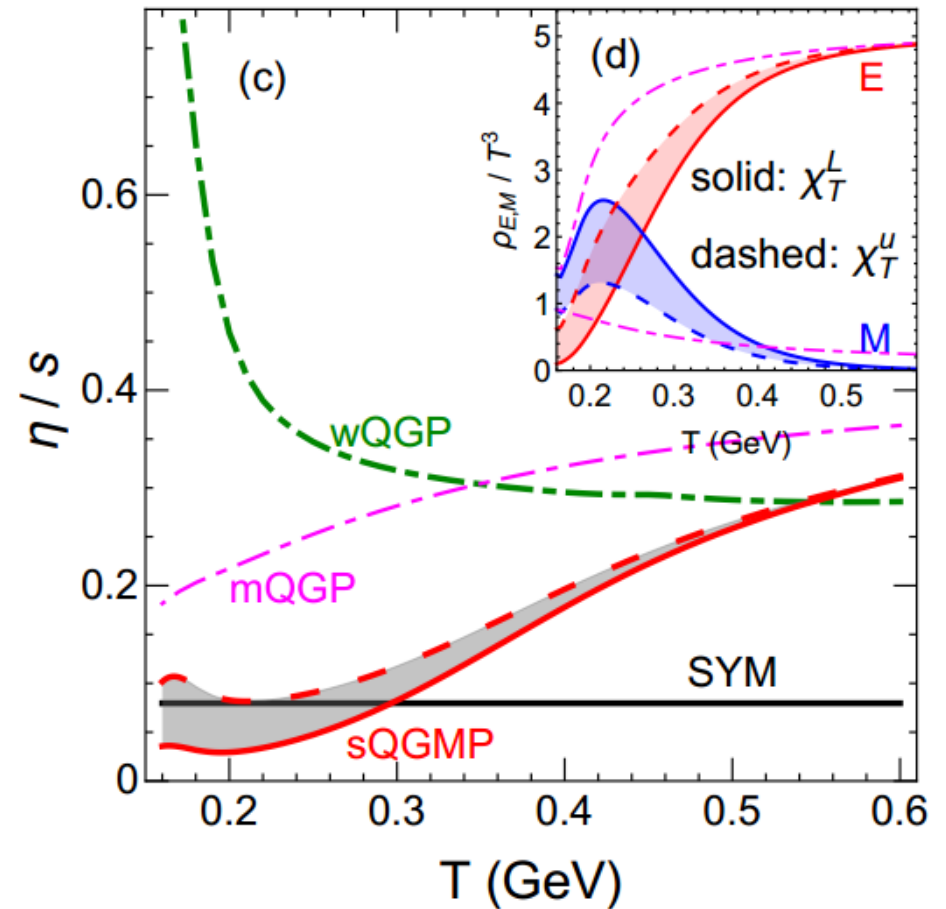
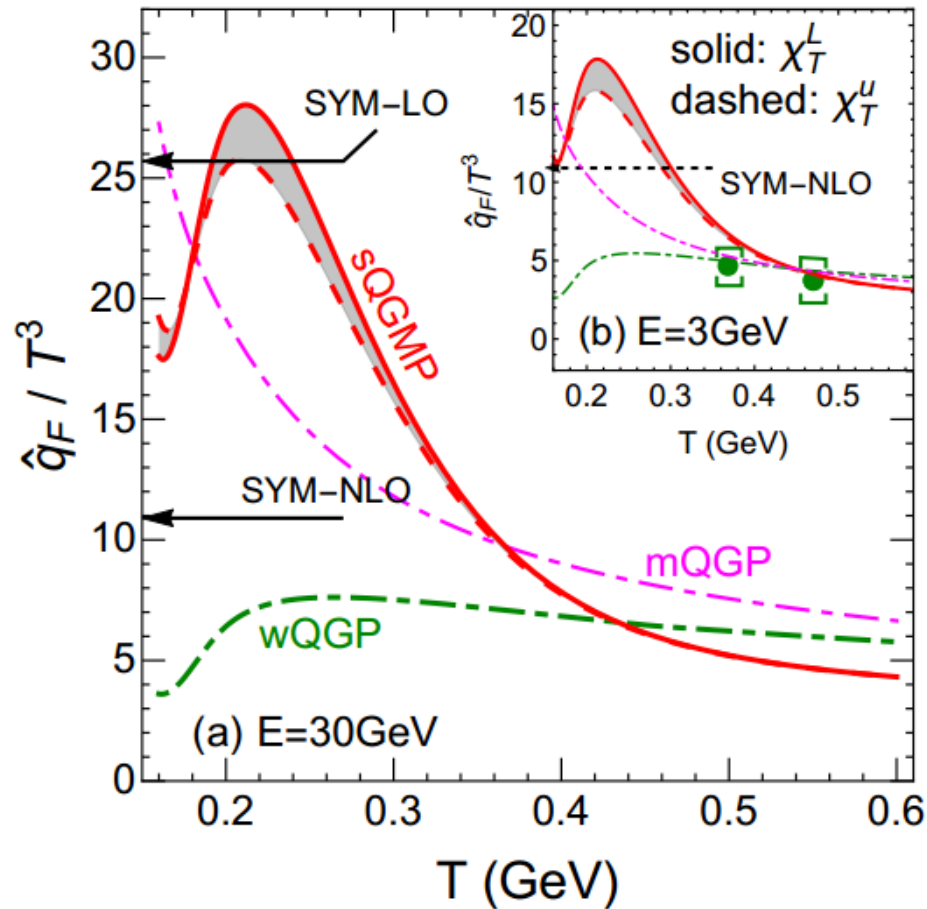
And ebe-vUSPH with
BBMG wQGP rates

We will Need further
observables to
Break this theory
degeneracy.
Dijet acoplanarity
may discriminate
very different internal
rates of the two
soft+hard
frameworks

$$\Gamma_{ab}(q_{\perp}, T) = \rho_b(T) d^2 \sigma_{ab}(T) / d^2 q_{\perp}$$

Compare sQGMP to wQGP and Zakharov's mQGP JETP Lett.(2015) where $q+g$ are not suppressed but a monopole component added.

The suppressed semi-QGP components of sQGMP require larger monopole density than in mQGP to compensate the loss $q+q$ component entropy to fit the lattice EOS P/T or $S(T)$



The mQGP monopole component is not big enough to reduce η/s close the SYM limit
 And it underpredicts jet v_2 data , in contrast to the CUJET 3 component semi-QGMP model

Extra Slides Below

distribution in the Sudakov resummation formalism as follows

$$\frac{d\sigma}{d\Delta\phi} = \sum_{a,b,c,d} \int p_{\perp\gamma} dp_{\perp\gamma} \int p_{\perp J} dp_{\perp J} \int dy_{\gamma} \int dy_J \int db$$

$$\times x_a f_a(x_a, \mu_b) x_b f_b(x_b, \mu_b) \frac{1}{\pi} \frac{d\sigma_{ab \rightarrow cd}}{d\hat{t}} b J_0(|\vec{q}_{\perp}| b) e^{-S(Q,b)}, \quad (1)$$

where J_0 is the Bessel function of the first kind, q_{\perp} is the transverse momentum imbalance between the photon and the jet $\vec{q}_{\perp} \equiv \vec{p}_{\perp\gamma} + \vec{p}_{\perp J}$, which takes into account both initial and final transverse momentum kicks from vacuum Sudakov radiations and medium gluon radiations. Here we define $x_{a,b} = \max(p_{\perp\gamma}, p_{\perp J})(e^{\pm y_{\gamma}} + e^{\pm y_J})/\sqrt{s_{NN}}$ as

The vacuum Sudakov factor $S_{pp}(Q, b)$ is defined as

$$S_{pp}(Q, b) = S_P(Q, b) + S_{NP}(Q, b) \quad (2)$$

where the perturbative S_P Sudakov factor depends on the incoming parton flavour and outgoing jet cone size. The perturbative Sudakov factors can be written as [35–37]

pQCD Vacuum Shower
$$S_P(Q, b) = \sum_{q,g} \int_{\mu_b^2}^{Q^2} \frac{d\mu^2}{\mu^2} \left[A \ln \frac{Q^2}{\mu^2} + B + D \ln \frac{1}{R^2} \right] \quad (3)$$

At the next-to-leading-log (NLL) accuracy, the coefficients can be expressed as $A = A_1 \frac{\alpha_s}{2\pi} + A_2 (\frac{\alpha_s}{2\pi})^2$, $B = B_1 \frac{\alpha_s}{2\pi}$ and $D = D_1 \frac{\alpha_s}{2\pi}$, with the value of individual terms given by the following table, where both A and B terms are summed over the corresponding incoming parton flavours.

	A_1	A_2	B_1	D_1
quark	C_F	$K \cdot C_F$	$-\frac{3}{2}C_F$	C_F
gluon	C_A	$K \cdot C_A$	$-2\beta C_A$	C_A

Here C_A and C_F are the gluon and quark Casimir factor, respectively. $\beta = \frac{11}{12} - \frac{N_f}{18}$, and $K = (\frac{67}{18} - \frac{\pi^2}{6})C_A - \frac{10}{9}N_f T_R$. $R^2 = \Delta\eta^2 + \Delta\phi^2$ represents the jet cone-size, which is set to match the experimental setup. The implementation of the non-perturbative Sudakov factor $S_{NP}(Q, b)$ follows the prescription given in Refs [61, 62]. In the Sudakov resummation formalism, following the usual b^* prescription, the factorization scale is set to be $\mu_b \equiv \frac{c_0}{b_{\perp}} \sqrt{1 + b_{\perp}^2/b_{max}^2}$,

Logarithmic approximations, quark form factors, and quantum chromodynamics

S. D. Ellis, N. Fleishon, and W. J. Stirling

1394

S. D. ELLIS, N. FLEISHON

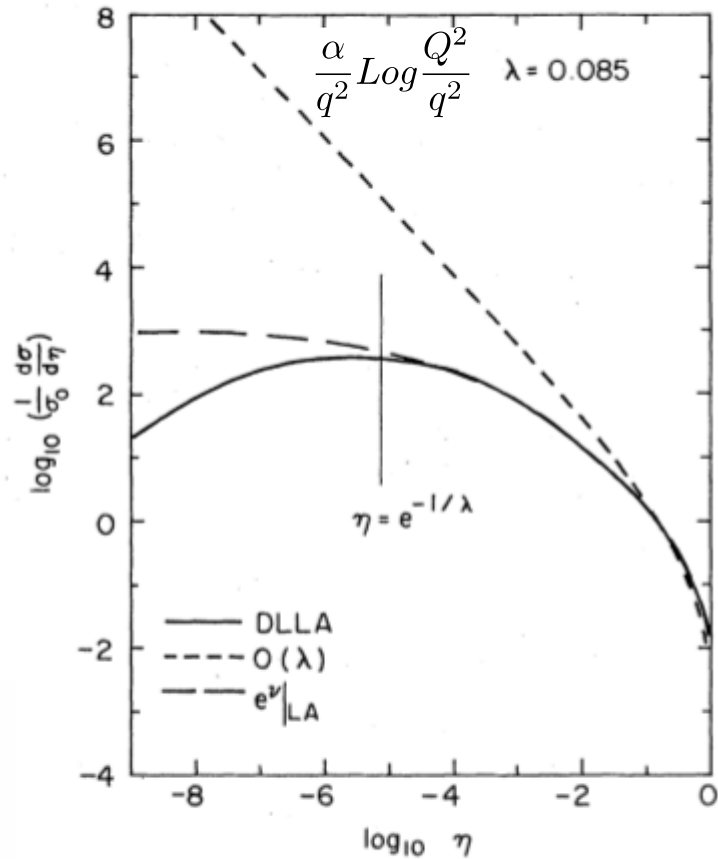


FIG. 4. Theoretical approximations to the cross section defined in the text. The long-dashed line is the soft logarithmic approximation [LA, (1), (2), (3)]. The solid line is the DLLA Eq. (2.12). The dashed line is the corresponding one-gluon contribution.

It is convenient to return to the general notation of the Introduction and define $\eta = Q_T^2/s$ and $\lambda = \alpha_s C_F/\pi$. Thus Eq. (2.11) can be written as

$$\begin{aligned} \frac{1}{\sigma_0} \frac{d\sigma}{d\eta} \Big|_{\text{DLLA}} &= \frac{\lambda}{\eta} \ln \frac{1}{\eta} \exp\left(-\frac{\lambda}{2} \ln^2 \eta\right) \theta(1-\eta) \\ &= \frac{d}{d\eta} F_{\text{DLLA}}(\eta) \theta(1-\eta) \end{aligned} \quad (2.12)$$

with $F_{\text{DLLA}}(\eta)$ identified from Eq. (1.1).

with $C_F = 4/3$, $T_R = 1/2$ and $N = 3$. It is instructive to see how the logarithms in b -space generate logarithms in q_T -space. For illustration, we take only the leading coefficient $A^{(1)} = 2C_F$ to be non-zero in $e^{S(b,Q^2)}$, and assume a fixed coupling α_s . This corresponds to

$$\frac{d\sigma}{dq_T^2} = \frac{\sigma_0}{2} \int_0^\infty b db J_0(q_T b) \exp\left[-\frac{\alpha_s C_F}{2\pi} \ln^2\left(\frac{Q^2 b^2}{b_0^2}\right)\right]. \quad (6)$$

The expressions are made more compact by defining new variables $\eta = q_T^2/Q^2$, $z = b^2 Q^2$, $\lambda = \alpha_s C_F/\pi$, $z_0 = 4 \exp(-2\gamma_E) = b_0^2$. Then

$$\frac{1}{\sigma_0} \frac{d\sigma}{d\eta} = \frac{1}{4} \int_0^\infty dz J_0(\sqrt{z\eta}) e^{-\frac{\lambda}{2} \ln^2(z/z_0)} \quad (7)$$

and we encounter the same expression as in [6], which describes the emission of soft and collinear gluons with transverse momentum conservation taken into account. The result

The conclusion is then that the *subleading logarithms* which arise from a correct treatment of transverse-momentum conservation can play a major role in filling in the zero at $\eta=0$ and obscuring the maximum which was present near $\ln 1/\eta \sim 1/\lambda$ in the DLLA. It is informative to di-